

1

2

3

4

5

6

7 **Novel Differences in Renal Gene Expression in a Diet Induced Obesity Model**

8

9

10 Victoria L. Halperin Kuhns, Jennifer L. Pluznick¹

11 Department of Physiology, Johns Hopkins University School of Medicine, Baltimore, MD 21205,
12 USA

13

14 ¹ Corresponding author: 725 N Wolfe St, WBSB 205, Department of Physiology, Johns Hopkins
15 University School of Medicine, Baltimore, MD 21205, USA 410 614 4660 Email:
16 jpluznick@jhmi.edu

17

18

19

20 Running title: Novel Changes in DIO Renal Gene Expression

21

22

23

24

25 **Abstract.**

26

27 Obesity is a significant risk factor for both chronic kidney disease and end stage renal disease.

28 To better understand disease development, we sought to identify novel genes differentially

29 expressed early in disease progression. We first confirmed that mice fed a high-fat (HF) diet

30 exhibit early signs of renal injury including hyperfiltration. We then performed RNA Seq using

31 renal cortex RNA from C57Bl/6 male mice fed either HF or control (Ctrl) diet. We identified 1134

32 genes differentially expressed in the cortex on HF versus Ctrl, of which 31 genes were selected

33 for follow up analysis. This included the 9 most upregulated, the 11 most downregulated, and 11

34 genes of interest (primarily sensory receptors and G proteins). qRT-PCR for these 31 genes

35 was performed on additional male renal cortex and medulla samples, and 11 genes (including

36 all 9 upregulated genes) were confirmed by qRT-PCR. We then examined expression of these

37 11 genes in Ctrl and HF male heart and liver samples, which demonstrated that these changes

38 are relatively specific to the renal cortex. These 11 genes were also examined in female renal

39 cortex, where we found that the expression changes seen in males on a HF diet are not

40 replicated in females – even when the females are started on diet sooner, in order to match

41 weight gain of the males. In sum, these data demonstrate that in a HF diet model of early

42 disease, novel transcriptional changes occur which are both sex-specific and specific to the

43 renal cortex.

44

45

46

47

48 **Introduction.**

49

50 Obesity is an international epidemic according to the World Health Organization(50).

51 Since 2002, more than 300 million people worldwide have been classified as obese, defined as
52 a body mass index (BMI) greater than 30(49). Approximately 38% of the adult population in the
53 United States were considered to be obese in 2013-2014, with a 35% incidence in men and a
54 40% incidence in women(28). Obesity is associated with many comorbidities, including kidney
55 disease(59, 109), cardiovascular disease(25), and diabetes(7). In addition, patients who are
56 morbidly obese, with BMI greater than 40, are 6 fold more likely to develop diabetes than lean
57 peers(19). Diabetes, in turn, can have additional detrimental effects on kidney function, which
58 can ultimately lead to end stage renal disease(110). Approximately 1 in 4 patients with diabetes
59 will experience a decline in renal function, which can lead to diabetic nephropathy (DN)(2). It
60 has been reported that the pathophysiology of DN is almost identical to that of obesity related
61 renal disease(68), and risk of kidney disease is doubled in the presence of both obesity and
62 diabetes(26). Disease progression in both conditions usually begins with hyperfiltration(13, 18,
63 38-40). Additional signs of disease include glomerulosclerosis, which is characterized by
64 increases in mesangial matrix deposition, basement membrane thickening(27), and collagen
65 infiltration of glomeruli(73). Despite current treatment options, roughly 50% of type 2 diabetic
66 patients will go on to develop end stage renal disease (30), which requires renal replacement
67 therapy: lifetime dialysis, or, transplant(29, 77). Obesity is also thought to be an independent
68 risk factor on development of end stage renal disease(42).

69 Previous studies have identified signaling pathways and proteins that are differentially
70 regulated in obesity related kidney disease. However, we hypothesized that there are likely
71 genes that play important roles in this disease but have not yet been studied. Thus, we aimed
72 to use an unbiased screen to identify genes differentially regulated in a model of diet induced

73 obesity (DIO) and early type 2 diabetes. In this study, we performed an RNASeq screen to
74 identify changes in gene expression that occur in the renal cortex in a mouse model of DIO. We
75 then worked to validate and further analyze these findings using real-time PCR for a sub-set of
76 these genes, and identified sex differences in these transcriptional changes. Because we are
77 particularly interested in roles for novel G-protein coupled receptors (GPCRs) in health and
78 disease, we also included genes related to these signaling pathways in our real-time PCR
79 follow-up studies. In sum, we have uncovered a novel set of differentially regulated genes in a
80 DIO mouse model. Ultimately, results from such screens may lead to better understanding of
81 disease progression, and/or may uncover novel targets for intervention and treatment of obesity
82 related kidney disease and/or DN.

83

84

85

86 **Methods and Materials**

87

88 **Mice.** All experiments were performed in compliance with the policies and procedures of the
89 Johns Hopkins Animal Care and Use Committee (ACUC). 11 week old male C57BL6/J DIO
90 mice (on diets from 6 weeks of age) were ordered from Jackson Labs (DIO high fat diet [HF,
91 60% fat diet] Cat#: 380050; DIO controls [Ctrl, 10% fat diet, 35% sucrose, Cat#: 380056]). Upon
92 arrival, mice were placed on respective diets (HF: Research Diets Inc. Cat# D12492, Ctrl:
93 Research Diets Inc. D12450J, 7% sucrose) for an additional 4 weeks, allowing for mice to be 15
94 weeks old at time of sacrifice (after 9 weeks on diet beginning at 6 weeks of age). One cohort
95 of HF and Ctrl mice were used for RNA Seq and follow up molecular experiments, while a
96 separate cohort of mice were used for physiological and histological studies. *Diet matched*
97 *females:* To match the dietary regimen of the male mice, female C57BL6/J mice were ordered
98 from Jackson Labs at 6 weeks of age (Cat# 000664) and were placed on either HF diet (n=5,
99 Research Diets Inc. Cat# D12492) or matched control diet (n=5, Research Diets Inc. D12450B,
100 35% sucrose) upon arrival. Ctrl mice were switched to Research Diets Inc. D12450J at 11
101 weeks, to match the treatment of the male cohort. *Weight matched females:* Female mice were
102 obtained from our strain matched C57BL6/J breeding colony and, starting from 3 weeks of age
103 (at weaning), were placed on either HF diet (n= 5, 60% kcal from fat, Research Diets Inc
104 #D12492) or control diet (n=4, Ctrl: 10% kcal from fat, 7% sucrose, Research Diets Inc
105 #D12450J). Mice from this colony were used in order to best control diet conditions upon
106 weaning. These mice remained on diet for another 12 weeks, and thus were also 15-weeks old
107 at the time of sacrifice. Mice were housed in approved facilities and were given access to food
108 and water *ad lib* with appropriate light/dark cycles in accordance with all regulations.

109

110 **Glucose Tolerance Test.** Mice were administered glucose tolerance tests prior to sacrifice
111 using established protocols.(86) In brief, mice were fasted overnight for approximately 16 hours,
112 and then administered an intraperitoneal injection of glucose using 5 μ l of 20% glucose solution
113 per 1 gram body weight. Blood glucose levels were measured using a Roche Accu-Chek Nano
114 glucometer prior to injection, then post injection at 15, 30, 60, 90, and 120 minutes. Data was
115 plotted and area under the curve measurements were calculated. A p<0.05 using a 2 tailed
116 unpaired Student's T Test was considered significant.

117

118 **Glomerular Filtration Rate.** Measurements were taken as described previously (84-86). In
119 brief, mice were anesthetized using inhaled Isoflurane in an enclosed chamber. Under light
120 sedation, hair was removed using an electric animal hair trimmer from a patch on the back.
121 Nair™ was then applied to the shaved region and immediately wiped off with damp gauze and
122 then rinsed with sterile water. Animals were then returned to their cages overnight. The
123 following day, mice were once again anesthetized using inhaled Isoflurane. Under light
124 sedation, a device was affixed to the shaved region using adhesive patches and then secured
125 with surgical tape. This device transcutaneously measures fluorescent compounds in the blood.
126 FITC conjugated sinistrin (an inulin analog) was then injected retroorbitally at a dose of
127 5.6mg/100 g body weight dissolved in sterile saline (0.9% NaCl) and clearance was monitored
128 for one hour post injection in real time via fluorescent signal decay. Data was then analyzed
129 using MPD Studio version Beta4 (Mannheim Pharma & Diagnostics, Amtsgericht Mannheim,
130 Germany). GFR was then calculated as volume per minute, by determining the rate constant
131 using the $t_{1/2}$ of the FITC-sinistrin decay curve as $\ln(2)/t_{1/2}$, as well as the extra cellular fluid
132 volume (ECVS) of each animal as 14616.8/100*body weight. GFR was ultimately calculated as
133 GFR (μ l/min) = rate constant*calculated ECVS. Details regarding these calculations have been
134 published previously(84, 85).

135

136 **Organ Harvesting.** Tissue samples were collected when mice were 15 weeks old ± 4 days.
137 Urine and feces were collected immediately prior to sacrifice, along with blood collected via tail
138 snip. Non-fasted blood glucose measurements were collected at this time using a Roche Accu-
139 Chek Nano glucometer. Mice were weighed, and then euthanized via CO₂ inhalation followed by
140 cervical dislocation. Liver, heart, visceral adipose, and right kidney tissues were harvested,
141 rinsed in 1x PBS, then flash frozen in liquid nitrogen and stored at -80°C. Left kidneys were
142 harvested, placed on ice, and then bisected using a razor blade. Each half was then bisected
143 again, and outer cortex and inner medulla were excised from each of the inner of the two
144 sections. Capsules were removed from all kidney samples prior to processing. In an additional
145 cohort of male mice fed both high fat and control diets described above, kidneys were instead
146 placed in 10% buffered formalin for histology studies.

147

148 **Histology.** Left kidneys stored in 10% buffered formalin were embedded in paraffin, and 5 µm
149 sections were either stained using Hematoxylin and eosin (H&E), picrosirius red (PSR), or
150 periodic acid-Schiff (PAS) using standard protocols (preparation and staining of sections
151 performed by AML Laboratories). Sections were then imaged at 10x and 40x using a Keyence
152 digital microscope (BZ-X700, Keyence Corp). H&E sections were imaged at 40x at 6 randomly
153 selected and evenly spaced fields of view around the outer cortex of each section. Each field of
154 view contained between 1 and 6 glomeruli. Glomerular size was quantified manually using
155 ImageJ. PSR imaging was performed in a similar manner. 10 fields of view containing between
156 2 and 5 glomeruli were used for quantification using the Keyence Hybrid Cell Count feature of
157 the BZ-X Analyzer software. Images were then de-identified. Glomeruli were individually
158 isolated from each image, and the amount of red staining was quantified using a set 'Hue'
159 threshold to encompass all red signal in the image. This threshold was then applied to all
160 glomeruli. Thresholding was also used to quantify the total amount of tissue in each glomerulus.
161 A ratio was then taken of the amount of red area versus the total tissue area. Samples were

162 then re-identified to allow for analysis. PAS imaging was performed in a similar manner to H&E
163 described above and minimal changes were observed in resulting glomeruli across both groups.

164

165 **Immunohistochemical Staining.** Paraffin sections were deparaffinized using xylenes followed
166 by rehydration in ethanol at 95%, 90%, 80%, 50%, and 35%. Antigen retrieval using citrate
167 buffer was performed, followed by permeabilization with 1% SDS in TBS for 5 minutes. Sections
168 were then washed, incubated in 3% hydrogen peroxide in methanol for 30 minutes, washed
169 again, and then blocked using 10% heat inactivated goat serum with 0.1% BSA in TBS. Next,
170 sections were stained for Collagen IV using anti-Collagen IV (Abcam #ab6586), which was
171 previously validated by (91, 106), at 1:50 or KIM-1 using anti-KIM-1 (R&D systems #AF1817),
172 which was previously validated by (IHC-P (45); WB: (48, 112)), at 1:100 in blocking buffer
173 overnight at 4°C. Samples were then washed and incubated with HRP conjugated secondary
174 antibody (Donkey anti-Rabbit-Peroxidase, Jackson ImmunoResearch #711-035-152; Donkey
175 anti-Goat Jackson ImmunoResearch #705-034-147) at 1:1000 for 1 hour at room temperature.
176 Samples were then washed twice with TBS for 5 minutes each, followed by 2 additional washes
177 of PBS. Sections were then developed using 3,3'-Diaminobenzidine (DAB) substrate solution
178 (Invitrogen #8801-4965) as per manufacturer's specifications for 10 minutes (Collagen IV), or 20
179 minutes (KIM-1), counterstained with hematoxylin for 45 seconds, washed and dehydrated in
180 the reverse of serial ethanol concentrations described above, followed by clearing with xylenes.
181 Slides were mounted using Histomount (Life Technologies #008030), visualized and total
182 Collagen IV-HRP signal per field of view was quantified as described above.

183

184 **Western Blots.** Right kidneys were cut in half and homogenized on ice using a Dounce
185 Homogenizer in 1x Radioimmunoprecipitation assay buffer (RIPA) buffer with protease inhibitors
186 and AEBSF. Samples were then sonicated on ice for 30 seconds at 20% amplitude for 3 bursts
187 with approximately a 5 minute rest in between each burst. Samples were then spun at 16,000g

188 for 15 minutes at 4°C. Equal amounts of protein were loaded under reducing conditions onto a
189 4-12% Bolt™ Bis-Tris Plus gel (Invitrogen #NW04125Box) and run as per manufacturer's
190 specifications using MOPS running buffer (Novex #B0001). The gel was then transferred using
191 the iBlot™2 Gel Transfer Device (Life Technologies #IB21001) using nitrocellulose membranes
192 and the default P0 transfer protocol as per manufacturer's specifications. Membranes were then
193 blocked in 1:2 Superblock® blocking buffer (Thermo Scientific #37580) in PBS for 2 hours at
194 room temperature. Membranes were incubated overnight in anti-KIM-1 at 1:200 in blocking
195 buffer. Next, membranes were washed with PBS-T, followed by incubation with peroxidase
196 conjugated secondary antibody at 1:10,000 in blocking buffer for 45 minutes at room
197 temperature. Membranes were washed and developed using SuperSignal™ West Pico PLUS
198 Chemiluminescent Substrate (Thermo Scientific #34579). Membranes were washed, and
199 stripped using Gentle ReView™ Stripping Buffer (Amresco #N552) for 20 minutes at room
200 temperature, washed again, then incubated with peroxidase conjugated GAPDH (Invitrogen
201 MA5-15738-HRP), washed again, and finally developed as above.

202

203 **RNA isolation and quality control.** Kidneys were homogenized using a mechanical
204 homogenizer and RNA was isolated using TRIzol®(Ambion™, Life Technologies
205 Cat#15596018) according to manufacturer's protocol. Phases were separated using Phase
206 Lock Gel tubes (5 Prime, Cat# 2302830) and following resuspension, samples were digested
207 using DNasel (Qiagen Cat#79254, manufacturer's specifications) for 30 minutes at room
208 temperature. RNA clean up was performed using 10 µl 3M sodium acetate at pH 5.2 with 400 µl
209 100% ethanol incubated for 2 minutes at room temperature. Samples were then spun at 16,000
210 x g for 10 minutes at 4°C. Ethanol was then evaporated and final samples were resuspended in
211 RNAse free molecular grade water. RNA quality was assessed using a BMG Labtech FLUOstar
212 Omega plate reader. Samples with an initial A260/A280>1.8 were processed using the RNA
213 Clean-up protocol from Qiagen's RNeasy mini kit. Samples utilized for RNA Seq had a RIN

214 number >9.5 (Aglient Bioanalyzer (2100 Expert (B.02.08.SI648)). Additional tissues were
215 homogenized using the MP FastPrep 24 homogenizer with the appropriate lysing matrix. Lysing
216 Matrix D (MP Biomedicals LLC, Cat#116913050) was used for liver samples for 3 runs at 6.0
217 m/s for 40 seconds, and for female kidney cortex samples for 2 runs at 6.0 m/s for 40 seconds.
218 Lysing Matrix SS (MP Biomedicals LLC Cat#116921050) was used for heart samples for 6 runs
219 at 6.0 m/s for 40 seconds. A 5 minute rest was performed between each run.

220

221 **Reverse transcriptase (RT)-PCR.** RNA was made into cDNA using the iScript™ cDNA
222 Synthesis Kit (Bio-Rad, #1708891) as per manufacturer's specifications. PCR was then
223 performed using HotStarTaq Master Mix Plus (Qiagen, #203443) using standard cycling
224 conditions (35 cycles) with primers annealing at 57°C unless otherwise specified. PCR primers
225 used were: Megalin (GTGTCTCCTTTGGCCCTGA, TCACAAGGTTGCGGTGTCT; 490 bp),
226 Nos1 (CTTCCGAAGTTTGCAACAGCGACAATT,
227 GGACTCAGATCTAAGGCAGTTGGTCACTTC, 472 bp, 63°C), UT-A1
228 (AGCAGGTCTTCCAGAACATGGC, AGATGGAGGGCCTTCAAGC, 330 bp), and β-actin
229 (CGGTTCCGATGCCCTGAGGC, AGGGTGAAAACGCAGCTCAGTAAC; 401 bp).

230

231 **RNA Seq Analysis.** In order to isolate mRNA from total RNA, samples were prepared using
232 TruSeq® Stranded Total RNA Sample Preparation Kit with Ribo-Zero Gold (Illumina, Cat#RS-
233 122-2303) as per manufacturer's specifications. RNA Seq analysis was performed using an
234 Illumina HiSeq 2000 for 200 cycles (100bp x 100bp) Paired End run. Output files were
235 converted from BCL to FASTQ using Illumina CASAVA 1.8.2 software default parameters.
236 Samples were analyzed by the Johns Hopkins Next Generation Sequencing branch of the
237 Experimental and Computational Genomics Core. Alignments were run using rsem-1.2.9 via the
238 'rsem-calculate-expression' module used with the following options: '--calc-ci,' '--output-
239 genome-bam,' '--paired-end,' and '--forward-prob 0.' Data was aligned to the mm10 mouse

240 reference genome; of note, reads were mapped to olfactory receptor genes using specified
241 coordinates.(46) Differential expression analysis was run using rsem-1.2.9 EBSeq via 'rsem-
242 run-ebseq' using an R script within rsem to run the EBSeq package. A false discovery rate of
243 0.05 was set as the threshold using the 'FDR_rate' script within 'rsem-control-FDR.' Each
244 sample gave between approximately 60 and 70 million reads. These reads were then aligned
245 using rsem to the mouse mm10 transcriptome database.

246

247

248 **Real-Time qPCR Follow up.** TaqMan arrays for targeted genes were used for the custom
249 Taqman Micro Fluidic Card array (Life Technologies, Format 32, Cat# 4346799). Each array
250 was defined as "gene specific" by the company and those genes for which "Best Coverage" was
251 available were chosen when possible. Cards were used to screen 16 samples and 2 negative
252 controls (1 no template control, 1 no reverse transcriptase control) according to manufacturer's
253 protocol. Samples included an expanded cohort of male cortex samples, in which 3 of each
254 group were animals that had been used for RNA Seq, plus 2 additional littermates (n=5 HF, n=5
255 Ctrl), and male medulla samples from the same animals used for RNA Seq (n=3 HF, n=3 Ctrl).
256 Roughly 24 hours prior to use on the array card, cDNA was made from 2 µg of RNA using the
257 High Capacity RNA-to-cDNA Kit (Life Technologies, Cat# 4387951). 1 µg of cDNA was used per
258 reservoir on the array card (2 reservoirs per sample, all cDNA used per sample per card) along
259 with recommended Master Mix (Life Technologies, Cat# 4440038). Individual assays for 11
260 genes were also obtained and screened against (a) heart and liver of the same male samples
261 screened using RNA Seq (n=3 per group per tissue), and (b) both weight-matched (n=3 HF, n=3
262 Ctrl) and diet-matched (n=4 HF, n=4 Ctrl) female renal cortex. All qRT-PCR reactions were run
263 using an Applied Biosystems 7900HT.

264

265 **Data Analysis of qRT-PCR.** qRT-PCR data was analyzed using Life Technologies
266 ExpressionSuite Software v1.0.3. Fold changes were obtained by grouping samples by tissue
267 type separated by sex, while ΔCT values for individual samples were obtained in a separate
268 analysis using no groups. Confirmation of differential expression was determined by a $p < 0.05$
269 using One Way ANOVA between male cortex Ctrl, male cortex HF, male medulla Ctrl, and male
270 medulla HF using SigmaPlot 11.0 (Systat Software, Inc.). Differential expression of confirmed
271 hits in other tissues was determined using 2 tailed unpaired T Tests were performed using
272 Microsoft Excel 2007 given $p < 0.05$ considered significant.

273

274 **KEGG Pathway analysis.** Differentially expressed genes were uploaded to DAVID
275 Bioinformatics Resouce version 6.7 (43, 44) using the “Functional Annotation” tool. A gene list
276 was uploaded and then analyzed by selecting the “Official_Gene_Symbol” from the menu and
277 then the *Mus musculus* background. Information was gathered on KEGG pathways and Gene
278 Ontology using default parameters.

279

280 **Results**

281

282 **HF Model.** After 9 weeks on their respective diets, males fed the HF diet weighed significantly
283 more than males fed a Ctrl diet (Figure 1A), and had elevated non-fasting blood glucose levels
284 as compared to controls (Figure 1B). Diet-matched female mice (treated the same as the
285 males) did not gain weight, in agreement with the literature(79, 111); however, weight-matched
286 females (who began the diet 3 weeks earlier, from weaning) did gain weight (Figure 1A). These
287 ‘weight-matched’ female mice were on the diet for a total of 12 weeks, and thus were age
288 matched at time of sacrifice, but were on the diet longer. This group was included to control for
289 weight gain on diet, since female mice on the diet for only 9 weeks failed to gain weight.
290 However, neither group of females demonstrated elevating non-fasting glucose levels (Figure
291 1B). Fasting glucose levels in males were significantly elevated as compared to age-matched
292 controls (Figure 1C, prior to glucose injection). HF males demonstrated impaired glucose
293 tolerance compared to Ctrl-fed males (Figure 1C&D), and an increase in glomerular filtration
294 rate (Figure 1E). No differences were observed between groups in urinary protein or glucose
295 concentration when samples were checked by dipstick. Kidney weight to body weight ratios
296 were measured in a small subset of these animals, revealing no change between the two
297 groups. Histological studies revealed a trend towards enlarged glomeruli in HF samples, as
298 demonstrated in H&E staining (Figure 2A-C). However, it should be noted that one extreme
299 outlier in the Ctrl samples was observed, which was greater than three standard deviations
300 above the mean. If this sample is omitted, then the resulting increase in glomerular size in the
301 HF samples reaches statistical significance. There was also a trend towards an increase in
302 glomerular collagen as indicated by picrosirius red staining (Figure 2D-F). When sections were
303 stained for Collagen IV, no statistically significant changes were seen between the two groups
304 (Figure 2G-I). There was no expression of the kidney injury molecular KIM-1 in either the Ctrl or
305 the HF samples by immunohistochemistry (Figure 2J-K) or by western blot (Figure 2L). As a

306 control for the KIM-1 western blot, a collaborator provided us with kidneys which had been
307 prepared as part of a separate study and subjected to ischemia for 30 minutes, then reperfusion
308 for 24 hours(16); these samples did yield a band for KIM-1. Finally, no change was seen in
309 mesangial matrix deposition, as determined by PAS staining (data not shown). Taken together,
310 these data demonstrate that these mice demonstrate a pre-diabetic phenotype with early signs
311 of kidney injury.

312

313 **RNA Seq.** In order to identify novel genes that are differentially expressed in the kidney on a
314 HF diet, we undertook an unbiased RNA Seq screen. Kidneys from 15 week-old male mice that
315 had been fed either control (Ctrl) or high fat (HF) diet for 9 weeks were dissected into cortex and
316 medulla, and RNA was isolated. Using RT-PCR, cortex samples were confirmed to be positive
317 for Megalin(11, 22) and Nos1(65, 92), while medulla samples were positive for Urea Transporter
318 1A(6, 102). All samples were positive for β-Actin. Using RNASeq, we analyzed a total of 4
319 animals per diet. Genes indicative of kidney injury(33, 104) were modestly increased in the HF
320 samples by RNASeq, including lipocalin 2 (2 fold), fibronectin (1.4 fold), and KIM-1 (1.3 fold),
321 although there was no increase in collagen IV (1.1 fold). However, none of these changes were
322 statistically significant with a false discovery rate < 0.05.

323 Investigation revealed 1134 genes that were differentially expressed between Ctrl and
324 HF samples. DAVID analysis(43, 44) using David 6.7 revealed that 353 genes clustered into 17
325 KEGG pathways. Pathways containing at least 4 genes are shown in Table 1. A complete list of
326 these genes and the corresponding fold changes can be found in the supplemental materials.
327 Networked interactions among these genes were not apparent (using the STRING protein-
328 protein interaction network(31, 89, 95)).

329

330 **Confirmation using qRT-PCR in male kidney tissue.** Of the 1134 differentially expressed
331 genes (DEGs), those genes with the most extreme fold changes were selected for validation

332 (Table 2). Genes selected had a posterior probability of equal expression (PPEE) less than
333 0.05, and a posterior probability of differential expression (PPDE) of greater than 0.95. PPEE
334 less than 5% indicates that the probability that a gene is equally expressed in both conditions in
335 less than 5%, while a PPDE of 95% implies the probability of that being differentially expressed
336 in both conditions is 95%. We selected the 11 DEGs with the greatest increase (Table 2A) or
337 greatest decrease (Table 2B), which were detected in all samples. Of those genes with greatest
338 positive fold change, we excluded from further analysis one pseudogene (Gm14435) and one
339 non-coding RNA (Gm15441). In addition, we included for follow-up genes of particular interest
340 to our group (i.e., sensory receptors and G proteins that were called as differentially expressed
341 with a false discovery rate < 0.05). These genes included 6 G-protein coupled receptors (3 with
342 known ligands, 3 orphan receptors), 2 proposed taste receptors, and 3 G proteins (Table 2C).
343 These additional DEGs of interest had PPEE values less than 0.01 and PPDE values greater
344 than 0.98 (Table 2C).

345
346 In order to validate the changes listed in Table 2, quantitative real time PCR (qRT-PCR) was
347 performed using a custom TaqMan low density array card composed of validated gene specific
348 assays on an expanded cohort of male renal cortex RNA (n=5 per group), as well as renal
349 medulla RNA from the same mice used for RNA seq analysis (n=3 per group). A list of
350 individual gene assays used can be found in Table 3.

351
352 Differential expression was confirmed by qRT-PCR for all up-regulated DEGs (Table 3A), while
353 only 2 down-regulated DEGs were significant by qRT-PCR (Table 3B) in male cortex samples.
354 Fold changes for other DEGs of interest were not significant by qRT-PCR (Table 3C). However,
355 it should be noted that even when qRT-PCR changes did not reach significance, the direction
356 and trend of the change was supported by the qRT-PCR data. Significance was determined
357 using one way ANOVA, unless otherwise indicated. Trends for fold change data appeared

358 similar between RNA Seq and qRT-PCR for up-regulated DEGs (Figure 3A) and down-
359 regulated DEGs (Figure 3B), as well as for the majority of the genes of interest (Figure 3C;
360 although not for Scnn1g, W1s or Gnat3). All genes listed had significant fold changes via RNA
361 Seq, while only a subset of these genes demonstrated significant fold changes via qRT-PCR as
362 indicated.

363

364 **Additional tissue screening using qRT-PCR.** Subsequently, we aimed to determine whether
365 the changes in gene expression confirmed by qRT-PCR (9 genes up-regulated and 2 down-
366 regulated) represented global changes in gene expression which occur with HF diet, or, whether
367 these changes were unique to the renal cortex. To address this, qRT-PCR (Table 4) was used
368 to screen additional tissues (heart, liver, renal medulla) for these 11 genes. The changes in
369 gene expression seen in the renal cortex were not replicated in the heart or in the liver,
370 indicating that the change in expression profile noted above is specific to the kidney (Table 4).
371 However, renal medulla samples demonstrated similar significant changes in 3 out of the 11
372 genes (Ctnn3, Slc7a12, **Gsta2**, p<0.05), with an additional 5 genes revealing the same trends,
373 though these values failed to reach significance (Table 4). Previously described fold changes as
374 per RNA Seq (column 2) and qRT-PCR data (column 3) for male cortex samples are shown for
375 comparison.

376

377 In addition, because our RNASeq and initial qRT-PCR was done using male samples, we also
378 examined these same 11 genes in female samples that were either diet matched or weight
379 matched. Diet matched female mice were treated exactly as the males in term of diet treatment.
380 As noted previously(79, 105, 111), the females failed to gain weight on HF diet (Figure 1A).
381 When female cortex samples were screened using qRT-PCR, only 1 gene demonstrated
382 statistically significant changes (Cyp2b10, p<0.05) with another 2 genes trending in the same
383 direction (Table 4). Since these females did not match the males in terms of weight gain, we

384 also analyzed the weight-matched females. Weight matched females demonstrated an
385 increase in a different gene (*Synpr*, $p<0.05$) with another significant change in *Ccl28* in the
386 opposite direction as observed in the males (Table 4). Thus, the pattern of changes in gene
387 expression seen in the male renal cortex is specific to males, and was not observed in either
388 group of females (Table 4).

389 **Discussion**

390 In this study, we sought to identify novel genes that are differentially regulated in the early
391 stages of obesity related kidney disease using an unbiased RNA Seq approach. We identified,
392 and subsequently confirmed by qRT-PCR, 11 genes which are differentially expressed in the
393 kidney but not in other metabolically active tissues using a diet induced obesity model.

394

395 *Diet induced obesity model.* In agreement with previous studies(5, 15, 93, 107, 108), we find
396 that diet induced obesity is a useful murine model for studying downstream kidney phenotypes
397 leading to diabetic renal disease. Particularly, these mice can be used to understand changes in
398 the kidney that demonstrate a phenotype with some of the hallmarks of both obesity related
399 kidney disease and DN including modest hyperfiltration(108), and a trend towards increases in
400 collagen infiltration(24). In addition, many patients with DN also have diet induced obesity, and
401 thus this model may better represent what happens in the patient. Focusing on changes early
402 in the development of disease may prove to be an effective strategy for therapy as intervention
403 at this stage could be the most helpful.

404

405 *Differentially expressed genes.* A few commonly studied targets were found to be modestly up-
406 regulated in the context of our RNA Seq screen, including angiotensin converting enzyme (ACE,
407 1.8 fold)(72, 103, 115), transforming growth factor, beta receptor II (TGF β II, 1.3 fold)(35, 75,
408 116), protein kinase C, alpha (PKC α 1.2 fold)(34, 60, 74), and MAD homolog 1 (Smad1, 1.2
409 fold)(1, 69, 97, 114). In addition, several of our top hits included targets of interest that have
410 been studied in the context of obesity or diabetes (although often in tissues other than the
411 kidney), as outlined below.

412

413 *Up-regulated genes.*

414 Of the up-regulated DEGs (Tables 2A, 3A), 4 have previously been associated with
415 diabetes, obesity, or both in the literature: Sorcs1, Ctxn3, Ccl228 and Cyp2b10. Sorcs1 has
416 strong associations with both type 1(76) and type 2(36) diabetes in GWAS performed in
417 humans, with SNPs associated with higher stimulated levels of plasma glucose and insulin
418 secretion in obese women with polycystic ovarian syndrome(41). Another study identified
419 Sorcs1 as a candidate gene responsible for beta cell degradation and impaired insulin
420 secretion(52). Animal models have revealed Ctxn3 to be up-regulated in kidneys in pups born to
421 either streptozotocin (STZ)-induced diabetic, salt induced hypertension, or high fructose fed
422 rats(96). Ccl28 has been shown to demonstrate anti-inflammatory effects on macrophages in
423 STZ-induced diabetic mouse kidneys(71), while an increase in activity of the Ccl28 receptor has
424 been shown to decrease food intake both normal(119) and high fat fed mice(47, 94). Finally,
425 increased expression of Cyp2b10 has been reported in STZ-induced diabetic livers of mice and
426 rats (levels could be corrected by insulin administration)(83), as well as in livers in a mouse
427 model of maturity onset diabetes of the young(21), and in livers of db/db mice(117), and ob/ob
428 mice fed high fat diet(20)

429 We have also identified 5 targets of particular interest: these are genes which were
430 significantly up-regulated in the kidneys of high fat fed animals by RNA Seq and qRT-PCR
431 (Tables 2A, 3A), but have never before been characterized in the context of diabetes, with
432 minimal reported links to obesity. Synaptoporin (Synpr) was initially thought only to be
433 expressed in the brain(23), particularly in synaptic vesicles(88), but has recently been shown to
434 be expressed in the kidney, specifically in glomeruli(61). Genes involved in vesicular membrane
435 maintenance have been shown to be upregulated in kidneys of $\text{Ins}2^{\text{Akita}}$ diabetic mice(82), which
436 may imply that Synpr is not only expressed in other types of vesicles, but also could be involved
437 in vesicular maintenance. Another novel gene implicated by our study is ATP12a, a non-gastric
438 H(+)-K(+)-ATPase particularly expressed in the cortical thick ascending limb(61), as well as in
439 the skin, the colon, and in placenta(51). ATP12a SNPs have been associated with left ventricle

440 dysfunction in the heart and could potentially be related to hypertension(56, 57). A third gene of
441 interest is Popdc3, one of the three isoforms belonging to the Popeye domain containing
442 proteins, which is known to be expressed in striated muscle(3). These proteins have a high
443 affinity for binding cAMP and may play a role in regulation of membrane potential(32).
444 Decreased Popdc3 expression has also been shown in gastric cancer(54, 66). Haploinsufficiency
445 of Popdc3 has been linked to defects in heart development in patients with Prader-Willi-like
446 phenotype who also present with obesity(14). This study concludes, however, that SIM1 seems
447 to be the gene responsible for obesity in these patients. Additionally, we identified LIM
448 homeobox protein 2 (Lhx2), a transcription factor, as a gene of interest. Lhx2 plays role in
449 neural development(67), and has also been associated with various cancers(55, 87, 113).
450 Interestingly, SNPs of Lhx2 have been associated with central obesity by GWAS in populations
451 of African decent(64), particularly waist circumference adjusted for BMI, with no apparent sex
452 differences. Finally, Ptpn5 is thought to be a brain specific phosphatase, which recognizes
453 mitogen-activated protein kinase (MAPK)-specific tyrosine phosphatases(8), and has been
454 linked to the pathology of Alzheimer's disease(90). Further studies are required to understand
455 the role of these proteins in the kidney.

456

457 *Down-regulated genes.*

458 Of the down-regulated DEGs (Tables 2B, 3B) 7 have been previously associated with
459 diabetes, obesity, or both: Slc7a12, Gsta2, Bhmt, Aqp4, Cyp2a5, Lipg, and Scd1. Of these 7
460 genes, only Gsta2 and Slc7a12 were confirmed by qRT-PCR in kidneys in our data set. Certain
461 polymorphisms of Gsta2 may lead to a decrease in prostaglandin synthesis(100). In cell culture
462 models, carnosic acid and carnosol (activators of the Keap1/Nrf2 pathway) have been reported
463 to induce glutathione metabolism by increasing expression of corresponding genes, including
464 Gsta2. This induction appears to block adipocyte differentiation in 3T3-L1 cells, providing
465 evidence for these compounds to potentially be used in the treatment of obesity(98). Also, in

466 contrast to our findings, Scl7a12 has been shown to be upregulated in kidneys of OVE26
467 mice.(58)

468

469 *Sensory Receptors and Signaling Proteins.*

470 Of the final group of DEGs (Table 2C), 3 GPCRs, 2 heterotrimeric G proteins, 1 sweet
471 taste receptor transduction protein, and 1 proposed salt taste receptor have been examined in
472 the context of obesity or in a diabetic context. GPR12 knock out mice exhibit obesity with normal
473 food intake, dyslipidemia, and hepatic steatosis(12), implying upregulation of this gene in our
474 study may be compensatory. Increased expression of Sucnr1 (GPR91) not only mediates renin
475 release and triggers MAPK activation, but also leads to diabetic nephropathy and renal fibrosis
476 in patients with type 2 diabetes(78, 101). Furthermore, Sucnr1 has been identified as potential
477 therapeutic target to ameliorate diabetic renal disease(4). Sucnr1 knock out mice fed a high fat
478 diet were initially protected from weight gain, but as the mice aged, weights were comparable to
479 wild type littermates but with increased white adipose tissue. These mice also failed to secrete
480 insulin and became progressively hyperglycemic, with no apparent pancreatic structural defects.
481 Authors concluded Sucnr1 might act as a sensor for dietary energy(70). In addition, GPR146
482 demonstrates interaction with proinsulin C-peptide(118).

483 Interestingly, the alpha subunit of one G protein, Gnai3 (Gi3), has been shown to be
484 affected by high glucose oxidative stress in the aorta of STZ-induced rats and vascular smooth
485 muscle cells(63). Gnai3 is expressed at low levels in adipocytes of both lean and obese
486 patients(53), as well as in the liver(17). Gna14 has also been associated with CpG islands, and
487 has demonstrated increased expression in livers of *A^{vY/a}* mice either fed high fat diet or
488 descended from mothers fed high fat diet(62).

489 Finally, there have been reports on the two genes associated with taste related to
490 obesity or diabetes. The gamma subunit of the proposed salt taste receptor ENaC, Scnn1g, is
491 well known as a key renal transporter, and has been extensively studied in the kidney, including

492 in models of obesity and diabetes such as the Zucker rat(10, 37, 81). Also, a recent study of
493 methylation patterns of peripheral white blood cells revealed a SNP of Gabbr1 to be associated
494 with CpG islands related to sweet taste transduction genes correlated with increased BMI,
495 which authors concluded to be a potential epigenetic mechanism for obesity(80).

496

497 *RNA Seq vs qRT-PCR.* Of the 31 genes of interest identified by RNA Seq, fold changes were
498 confirmed in 11 of these genes by qRT-PCR. The fold changes which were replicated by qRT-
499 PCR were often those of larger magnitudes (>5 fold, Table 2A), or for genes which are highly
500 expressed (Gsta2, FPKM >200 in Ctrl, Table 2B). The remaining genes had either more modest
501 expression levels, or the qRT-PCR probe specificity was limited, as in the case of Cyp2b5,
502 which also cross-reacts with Cyp2b4.

503

504 *Differences between males and females.* Males and females are known to respond differently to
505 treatment to induce obesity(9, 79, 99, 105, 111). Our study has shown that females can gain
506 comparable weight to males if they are started on the diet 3 weeks earlier; however, even with
507 the longer diet regimen, the females did not exhibit an increase in random plasma glucose
508 (Figure 1). Similarly, the overall changes in gene expression profile were not observed in the
509 female animals in either the diet matched or the weight matched conditions. In future studies, it
510 would be beneficial to better understand these sex differences.

511

512 In conclusion, we have identified a novel set of genes that are differentially regulated
513 early in the development of obesity related kidney disease in a pre-diabetic context. It is
514 important to note that these experiments were performed in one particular model; in the future it
515 is crucial to address these findings in a more specific type 2 diabetes murine model, such as
516 C57BL6 *db/db*, C57BLKS *db/db*, BTBR *ob/ob*(5, 15) or even a type 1 model, such as STZ-
517 induced diabetes. Further studies are also required to understand how changes in expression

518 levels of these genes occur throughout the course of obesity related kidney disease, as well as
519 to determine the role these genes play in the context of DN, either in development of the
520 disease or in response to it.

521

522

523

524 **Acknowledgements**

525 We are grateful to the members of the Johns Hopkins Sidney Kimmel Cancer Center Next
526 Generation Sequencing Core, especially Alyza Skaist and Jennifer Meyers, as well as Dr.
527 Liliana Florea and Corina Antonescu of the Johns Hopkins Computational Biology Consulting
528 Core. In addition, we would like to thank the lab of Dr. Will Wong, as well as Dr. Blythe Shepard
529 and members of the Pluznick Lab for their advice and helpful discussions. We are also grateful
530 to Dr. Darren Logan for guidance on correctly aligning olfactory receptors genes to RNASeq
531 data. In addition, we are grateful to Dr. Hamid Rabb and the members of his laboratory for the
532 generous gift of kidneys subjected to ischemia-reperfusion injury. This work was in part
533 supported by a Computational Expertise Grant from the Johns Hopkins Computational Biology
534 Consulting Core.

535

536 References
537

- 538 1. **Abe H, Matsubara T, Iehara N, Nagai K, Takahashi T, Arai H, Kita T, and Doi T.**
539 Type IV collagen is transcriptionally regulated by Smad1 under advanced glycation end
540 product (AGE) stimulation. *The Journal of biological chemistry* 279: 14201-14206, 2004.
541 2. **Afkarian M, Zelnick LR, Hall YN, and et al.** Clinical manifestations of kidney
542 disease among us adults with diabetes, 1988-2014. *JAMA* 316: 602-610, 2016.
543 3. **Andrée B, Hillemann T, Kessler-Icekson G, Schmitt-John T, Jockusch H, Arnold**
544 **H-H, and Brand T.** Isolation and Characterization of the Novel Popeye Gene Family
545 Expressed in Skeletal Muscle and Heart. *Developmental Biology* 223: 371-382, 2000.
546 4. **Ariza AC, Deen PM, and Robben JH.** The succinate receptor as a novel therapeutic
547 target for oxidative and metabolic stress-related conditions. *Frontiers in endocrinology* 3:
548 22, 2012.
549 5. **Azushima K, Gurley SB, and Coffman TM.** Modelling diabetic nephropathy in mice.
550 *Nature reviews Nephrology* 2017.
551 6. **Bankir LT, and Trinh-Trang-Tan MM.** Renal urea transporters. Direct and indirect
552 regulation by vasopressin. *Experimental physiology* 85 Spec No: 243S-252S, 2000.
553 7. **Barnes AS.** The epidemic of obesity and diabetes: trends and treatments. *Texas*
554 *Heart Institute journal* 38: 142-144, 2011.
555 8. **Barr AJ, and Knapp S.** MAPK-specific tyrosine phosphatases: new targets for drug
556 discovery? *Trends in pharmacological sciences* 27: 525-530, 2006.
557 9. **Begin-Heick N.** Of mice and women: the beta 3-adrenergic receptor leptin and
558 obesity. *Biochemistry and cell biology = Biochimie et biologie cellulaire* 74: 615-622, 1996.
559 10. **Bickel CA, Knepper MA, Verbalis JG, and Ecelbarger CA.** Dysregulation of renal
560 salt and water transport proteins in diabetic Zucker rats. *Kidney Int* 61: 2099-2110, 2002.
561 11. **Birn H, Willnow TE, Nielsen R, Norden AG, Bonsch C, Moestrup SK, Nexo E, and**
562 **Christensen EI.** Megalin is essential for renal proximal tubule reabsorption and
563 accumulation of transcobalamin-B(12). *American journal of physiology Renal physiology*
564 282: F408-416, 2002.
565 12. **Bjursell M, Gerdin AK, Jonsson M, Surve VV, Svensson L, Huang XF, Tornell J,**
566 **and Bohlooly YM.** G protein-coupled receptor 12 deficiency results in dyslipidemia and
567 obesity in mice. *Biochemical and biophysical research communications* 348: 359-366, 2006.
568 13. **Blantz RC, and Singh P.** Glomerular and tubular function in the diabetic kidney.
569 *Advances in chronic kidney disease* 21: 297-303, 2014.
570 14. **Bonaglia MC, Ciccone R, Gimelli G, Gimelli S, Marelli S, Verheij J, Giorda R,**
571 **Grasso R, Borgatti R, Pagone F, Rodriguez L, Martinez-Frias ML, van Ravenswaaij C,**
572 **and Zuffardi O.** Detailed phenotype-genotype study in five patients with chromosome
573 6q16 deletion: narrowing the critical region for Prader-Willi-like phenotype. *European*
574 *journal of human genetics : EJHG* 16: 1443-1449, 2008.
575 15. **Breyer MD, Bottinger E, Brosius FC, 3rd, Coffman TM, Harris RC, Heilig CW, and**
576 **Sharma K.** Mouse models of diabetic nephropathy. *Journal of the American Society of*
577 *Nephrology : JASN* 16: 27-45, 2005.
578 16. **Burne MJ, Daniels F, El Ghadour A, Mauiyyedi S, Colvin RB, O'Donnell MP, and**
579 **Rabb H.** Identification of the CD4(+) T cell as a major pathogenic factor in ischemic acute
580 renal failure. *The Journal of clinical investigation* 108: 1283-1290, 2001.

- 581 17. **Caro JF, Raju MS, Caro M, Lynch CJ, Poulos J, Exton JH, and Thakkar JK.** Guanine
582 nucleotide binding regulatory proteins in liver from obese humans with and without type II
583 diabetes: evidence for altered "cross-talk" between the insulin receptor and Gi-proteins.
584 *Journal of cellular biochemistry* 54: 309-319, 1994.
- 585 18. **Chagnac A, Herman M, Zingerman B, Erman A, Rozen-Zvi B, Hirsh J, and Gafter**
586 U. Obesity-induced glomerular hyperfiltration: its involvement in the pathogenesis of
587 tubular sodium reabsorption. *Nephrology, dialysis, transplantation : official publication of*
588 *the European Dialysis and Transplant Association - European Renal Association* 23: 3946-
589 3952, 2008.
- 590 19. **Chan JM, Rimm EB, Colditz GA, Stampfer MJ, and Willett WC.** Obesity, fat
591 distribution, and weight gain as risk factors for clinical diabetes in men. *Diabetes care* 17:
592 961-969, 1994.
- 593 20. **Cheng Q, Aleksunes LM, Manautou JE, Cherrington NJ, Scheffer GL, Yamasaki H,**
594 **and Slitt AL.** Drug-metabolizing enzyme and transporter expression in a mouse model of
595 diabetes and obesity. *Molecular pharmacetics* 5: 77-91, 2008.
- 596 21. **Cheung C, Akiyama TE, Kudo G, and Gonzalez FJ.** Hepatic expression of
597 cytochrome P450s in hepatocyte nuclear factor 1-alpha (HNF1alpha)-deficient mice.
598 *Biochemical pharmacology* 66: 2011-2020, 2003.
- 599 22. **Christensen EI, and Birn H.** Megalin and cubilin: multifunctional endocytic
600 receptors. *Nature reviews Molecular cell biology* 3: 256-266, 2002.
- 601 23. **Dai J, Ji C, Gu S, Wu Q, Wang L, Xu J, Zeng L, Ye X, Yin G, Xie Y, and Mao Y.** Cloning
602 and sequence analysis of the human cDNA encoding the synaptoporin (delta), a highly
603 conservative synaptic vesicle protein. *Molecular biology reports* 30: 185-191, 2003.
- 604 24. **Deji N, Kume S, Araki S, Soumura M, Sugimoto T, Isshiki K, Chin-Kanasaki M,**
605 **Sakaguchi M, Koya D, Haneda M, Kashiwagi A, and Uzu T.** Structural and functional
606 changes in the kidneys of high-fat diet-induced obese mice. *American journal of physiology*
607 *Renal physiology* 296: F118-126, 2009.
- 608 25. **Eckel RH.** Obesity and heart disease: a statement for healthcare professionals from
609 the Nutrition Committee, American Heart Association. *Circulation* 96: 3248-3250, 1997.
- 610 26. **Ejerblad E, Fored CM, Lindblad P, Fryzek J, McLaughlin JK, and Nyren O.** Obesity
611 and risk for chronic renal failure. *Journal of the American Society of Nephrology : JASN* 17:
612 1695-1702, 2006.
- 613 27. **Fioretto P, and Mauer M.** HISTOPATHOLOGY OF DIABETIC NEPHROPATHY.
614 *Seminars in nephrology* 27: 195-207, 2007.
- 615 28. **Flegal KM, Kruszon-Moran D, Carroll MD, Fryar CD, and Ogden CL.** Trends in
616 Obesity Among Adults in the United States, 2005 to 2014. *JAMA* 315: 2284-2291, 2016.
- 617 29. **Fleming GM.** Renal replacement therapy review: Past, present and future.
618 *Organogenesis* 7: 2-12, 2011.
- 619 30. **Fox CS, Matsushita K, Woodward M, Bilo HJG, Chalmers J, Lambers Heerspink**
620 **HJ, Lee BJ, Perkins RM, Rossing P, Sairenchi T, Tonelli M, Vassalotti JA, Yamagishi K,**
621 **Coresh J, de Jong PE, Wen C-P, Nelson RG, and for the Chronic Kidney Disease**
622 **Prognosis C.** Associations of kidney disease measures with mortality and end-stage renal
623 disease in individuals with and without diabetes: a meta-analysis. *Lancet* 380: 1662-1673,
624 2012.
- 625 31. **Franceschini A, Szklarczyk D, Frankild S, Kuhn M, Simonovic M, Roth A, Lin J,**
626 **Minguez P, Bork P, von Mering C, and Jensen LJ.** STRING v9.1: protein-protein

- 627 interaction networks, with increased coverage and integration. *Nucleic acids research* 41:
628 D808-815, 2013.
- 629 32. **Froese A, Breher SS, Waldeyer C, Schindler RF, Nikolaev VO, Rinne S,**
630 **Wischmeyer E, Schlueter J, Becher J, Simrick S, Vauti F, Kuhtz J, Meister P, Kreissl S,**
631 **Torlopp A, Liebig SK, Laakmann S, Muller TD, Neumann J, Stieber J, Ludwig A, Maier**
632 **SK, Decher N, Arnold HH, Kirchhof P, Fabritz L, and Brand T.** Popeye domain containing
633 proteins are essential for stress-mediated modulation of cardiac pacemaking in mice. *The*
634 *Journal of clinical investigation* 122: 1119-1130, 2012.
- 635 33. **Genovese F, Manresa AA, Leeming DJ, Karsdal MA, and Boor P.** The extracellular
636 matrix in the kidney: a source of novel non-invasive biomarkers of kidney fibrosis?
637 *Fibrogenesis & tissue repair* 7: 4, 2014.
- 638 34. **Geraldes P, and King GL.** Activation of protein kinase C isoforms and its impact on
639 diabetic complications. *Circulation research* 106: 1319-1331, 2010.
- 640 35. **Goldfarb S, and Ziyadeh FN.** TGF-beta: a crucial component of the pathogenesis of
641 diabetic nephropathy. *Transactions of the American Clinical and Climatological Association*
642 112: 27-32; discussion 33, 2001.
- 643 36. **Goodarzi MO, Lehman DM, Taylor KD, Guo X, Cui J, Quinones MJ, Clee SM,**
644 **Yandell BS, Blangero J, Hsueh WA, Attie AD, Stern MP, and Rotter JI.** SORCS1: a novel
645 human type 2 diabetes susceptibility gene suggested by the mouse. *Diabetes* 56: 1922-
646 1929, 2007.
- 647 37. **Guan Y, Hao C, Cha DR, Rao R, Lu W, Kohan DE, Magnuson MA, Redha R, Zhang**
648 **Y, and Breyer MD.** Thiazolidinediones expand body fluid volume through PPARgamma
649 stimulation of ENaC-mediated renal salt absorption. *Nature medicine* 11: 861-866, 2005.
- 650 38. **Hall PM.** Prevention of Progression in Diabetic Nephropathy. *Diabetes Spectrum* 19:
651 18, 2006.
- 652 39. **Henegar JR, Bigler SA, Henegar LK, Tyagi SC, and Hall JE.** Functional and
653 structural changes in the kidney in the early stages of obesity. *Journal of the American*
654 *Society of Nephrology : JASN* 12: 1211-1217, 2001.
- 655 40. **Hostetter TH.** Hyperfiltration and glomerulosclerosis. *Semin Nephrol* 23: 194-199,
656 2003.
- 657 41. **Hrovat A, Kravos NA, Goricar K, Jensterle Sever M, Janez A, and Dolzan V.**
658 SORCS1 polymorphism and insulin secretion in obese women with polycystic ovary
659 syndrome. *Gynecological endocrinology : the official journal of the International Society of*
660 *Gynecological Endocrinology* 32: 395-398, 2016.
- 661 42. **Hsu CY, McCulloch CE, Iribarren C, Darbinian J, and Go AS.** Body mass index and
662 risk for end-stage renal disease. *Annals of internal medicine* 144: 21-28, 2006.
- 663 43. **Huang DW, Sherman BT, and Lempicki RA.** Bioinformatics enrichment tools:
664 paths toward the comprehensive functional analysis of large gene lists. *Nucleic acids*
665 *research* 37: 1-13, 2009.
- 666 44. **Huang DW, Sherman BT, and Lempicki RA.** Systematic and integrative analysis of
667 large gene lists using DAVID bioinformatics resources. *Nat Protocols* 4: 44-57, 2008.
- 668 45. **Humphreys BD, Czerniak S, DiRocco DP, Hasnain W, Cheema R, and Bonventre**
669 **JV.** Repair of injured proximal tubule does not involve specialized progenitors. *Proceedings*
670 *of the National Academy of Sciences of the United States of America* 108: 9226-9231, 2011.
- 671 46. **Ibarra-Soria X, Levitin MO, Saraiva LR, and Logan DW.** The olfactory
672 transcriptomes of mice. *PLoS genetics* 10: e1004593, 2014.

- 673 47. **Irwin N, Montgomery IA, and Flatt PR.** Comparison of the metabolic effects of
674 sustained CCK1 receptor activation alone and in combination with upregulated leptin
675 signalling in high-fat-fed mice. *Diabetologia* 56: 1425-1435, 2013.
- 676 48. **Ishida R, Kami D, Kusaba T, Kirita Y, Kishida T, Mazda O, Adachi T, and Gojo S.**
677 Kidney-specific Sonoporation-mediated Gene Transfer. *Molecular therapy : the journal of*
678 *the American Society of Gene Therapy* 24: 125-134, 2016.
- 679 49. **IUNS.** The Global Challenge of Obesity and the International Obesity Task Force
680 International Union of Nutritional Sciences. <http://www.iuns.org/resources/the-global-challenge-of-obesity-and-the-international-obesity-task-force/>. [2017].
- 682 50. **James WP.** WHO recognition of the global obesity epidemic. *Int J Obes (Lond)* 32
683 Suppl 7: S120-126, 2008.
- 684 51. **Johansson M, Jansson T, Pestov NB, and Powell TL.** Non-gastric H⁺/K⁺ ATPase is
685 present in the microvillous membrane of the human placental syncytiotrophoblast.
686 *Placenta* 25: 505-511, 2004.
- 687 52. **Joost HG, and Schurmann A.** The genetic basis of obesity-associated type 2
688 diabetes (diabesity) in polygenic mouse models. *Mammalian genome : official journal of the*
689 *International Mammalian Genome Society* 25: 401-412, 2014.
- 690 53. **Kaartinen JM, LaNoue KF, and Ohisalo JJ.** Quantitation of inhibitory G-proteins in
691 fat cells of obese and normal-weight human subjects. *Biochimica et biophysica acta* 1201:
692 69-75, 1994.
- 693 54. **Kim M, Jang H-R, Haam K, Kang T-W, Kim J-H, Kim S-Y, Noh S-M, Song K-S, Cho**
694 **J-S, Jeong H-Y, Kim JC, Yoo H-S, and Kim YS.** Frequent silencing of popeye domain-
695 containing genes, BVES and POPDC3 , is associated with promoter hypermethylation in
696 gastric cancer. *Carcinogenesis* 31: 1685-1693, 2010.
- 697 55. **Kim MS, Lee J, Oh T, Moon Y, Chang E, Seo KS, Hoehn BD, An S, and Lee JH.**
698 Genome-wide identification of OTP gene as a novel methylation marker of breast cancer.
699 *Oncology reports* 27: 1681-1688, 2012.
- 700 56. **Kinoshita K, Ashenagar MS, Tabuchi M, and Higashino H.** Whole rat DNA array
701 survey for candidate genes related to hypertension in kidneys from three spontaneously
702 hypertensive rat substrains at two stages of age and with hypotensive induction caused by
703 hydralazine hydrochloride. *Experimental and therapeutic medicine* 2: 201-212, 2011.
- 704 57. **Knez J, Salvi E, Tikhonoff V, Stolarz-Skrzypek K, Ryabikov A, Thijs L, Braga D,**
705 **Kloch-Badelek M, Malyutina S, Casiglia E, Czarnecka D, Kawecka-Jaszcz K, Cusi D,**
706 **Nawrot T, Staessen JA, and Kuznetsova T.** Left ventricular diastolic function associated
707 with common genetic variation in ATP12A in a general population. *BMC medical genetics*
708 15: 121, 2014.
- 709 58. **Komers R, Xu B, Fu Y, McClelland A, Kantharidis P, Mittal A, Cohen HT, and**
710 **Cohen DM.** Transcriptome-based analysis of kidney gene expression changes associated
711 with diabetes in OVE26 mice, in the presence and absence of losartan treatment. *PLOS ONE*
712 9: e96987, 2014.
- 713 59. **Kopple JD.** Obesity and chronic kidney disease. *Journal of renal nutrition : the official*
714 *journal of the Council on Renal Nutrition of the National Kidney Foundation* 20: S29-30,
715 2010.
- 716 60. **Koya D, and King GL.** Protein kinase C activation and the development of diabetic
717 complications. *Diabetes* 47: 859-866, 1998.

- 718 61. **Lee JW, Chou CL, and Knepper MA.** Deep Sequencing in Microdissected Renal
719 Tubules Identifies Nephron Segment-Specific Transcriptomes. *Journal of the American
720 Society of Nephrology : JASN* 26: 2669-2677, 2015.
- 721 62. **Li CC, Young PE, Maloney CA, Eaton SA, Cowley MJ, Buckland ME, Preiss T,
722 Henstridge DC, Cooney GJ, Febbraio MA, Martin DI, Cropley JE, and Suter CM.** Maternal
723 obesity and diabetes induces latent metabolic defects and widespread epigenetic changes
724 in isogenic mice. *Epigenetics* 8: 602-611, 2013.
- 725 63. **Li Y, Descorbeth M, and Anand-Srivastava MB.** Role of oxidative stress in high
726 glucose-induced decreased expression of G_i/α proteins and adenylyl
727 cyclase signaling in vascular smooth muscle cells. *American Journal of Physiology - Heart
728 and Circulatory Physiology* 294: H2845, 2008.
- 729 64. **Liu CT, Monda KL, Taylor KC, Lange L, Demerath EW, Palmas W, Wojczynski
730 MK, Ellis JC, Vitolins MZ, Liu S, Papanicolaou GJ, Irvin MR, Xue L, Griffin PJ, Nalls MA,
731 Adeyemo A, Liu J, Li G, Ruiz-Narvaez EA, Chen WM, Chen F, Henderson BE, Millikan
732 RC, Ambrosone CB, Strom SS, Guo X, Andrews JS, Sun YV, Mosley TH, Yanek LR,
733 Shriner D, Haritunians T, Rotter JI, Speliotis EK, Smith M, Rosenberg L, Mychaleckyj J,
734 Nayak U, Spruill I, Garvey WT, Pettaway C, Nyante S, Bandera EV, Britton AF,
735 Zonderman AB, Rasmussen-Torvik LJ, Chen YD, Ding J, Lohman K, Kritchevsky SB,
736 Zhao W, Peyser PA, Kardia SL, Kabagambe E, Broeckel U, Chen G, Zhou J, Wassertheil-
737 Smoller S, Neuhouser ML, Rampersaud E, Psaty B, Kooperberg C, Manson JE, Kuller
738 LH, Ochs-Balcom HM, Johnson KC, Sucheston L, Ordovas JM, Palmer JR, Haiman CA,
739 McKnight B, Howard BV, Becker DM, Bielak LF, Liu Y, Allison MA, Grant SF, Burke GL,
740 Patel SR, Schreiner PJ, Borecki IB, Evans MK, Taylor H, Sale MM, Howard V, Carlson
741 CS, Rotimi CN, Cushman M, Harris TB, Reiner AP, Cupples LA, North KE, and Fox CS.
742 Genome-wide association of body fat distribution in African ancestry populations suggests
743 new loci. *PLoS genetics* 9: e1003681, 2013.**
- 744 65. **Lu Y, Wei J, Stec DE, Roman RJ, Ge Y, Cheng L, Liu EY, Zhang J, Hansen PB, Fan F,
745 Juncos LA, Wang L, Pollock J, Huang PL, Fu Y, Wang S, and Liu R.** Macula Densa Nitric
746 Oxide Synthase 1beta Protects against Salt-Sensitive Hypertension. *Journal of the American
747 Society of Nephrology : JASN* 27: 2346-2356, 2016.
- 748 66. **Luo D, Lu ML, Zhao GF, Huang H, Zheng MY, Chang J, Lv L, and Luo JB.** Reduced
749 Popdc3 expression correlates with high risk and poor survival in patients with gastric
750 cancer. *World journal of gastroenterology* 18: 2423-2429, 2012.
- 751 67. **Marcos-Mondéjar P, Peregrín S, Li JY, Carlsson L, Tole S, and López-Bendito G.**
752 The Lhx2 Transcription Factor Controls Thalamocortical Axonal
753 Guidance by Specific Regulation of Robo1 and Robo2 Receptors. *The Journal of
754 Neuroscience* 32: 4372, 2012.
- 755 68. **Maric-Bilkan C.** Obesity and diabetic kidney disease. *The Medical clinics of North
756 America* 97: 59-74, 2013.
- 757 69. **Matsubara T, Abe H, Arai H, Nagai K, Mima A, Kanamori H, Sumi E, Takahashi
758 T, Matsuura M, Iehara N, Fukatsu A, Kita T, and Doi T.** Expression of Smad1 is directly
759 associated with mesangial matrix expansion in rat diabetic nephropathy. *Lab Invest* 86:
760 357-368, 2006.
- 761 70. **McCreath KJ, Espada S, Galvez BG, Benito M, de Molina A, Sepulveda P, and
762 Cervera AM.** Targeted disruption of the SUCNR1 metabolic receptor leads to dichotomous
763 effects on obesity. *Diabetes* 64: 1154-1167, 2015.

- 764 71. **Miyamoto S, Shikata K, Miyasaka K, Okada S, Sasaki M, Kodera R, Hirota D,**
 765 **Kajitani N, Takatsuka T, Kataoka HU, Nishishita S, Sato C, Funakoshi A, Nishimori H,**
 766 **Uchida HA, Ogawa D, and Makino H.** Cholecystokinin plays a novel protective role in
 767 diabetic kidney through anti-inflammatory actions on macrophage: anti-inflammatory
 768 effect of cholecystokinin. *Diabetes* 61: 897-907, 2012.
- 769 72. **Myauchi E, Hosojima H, and Morimoto S.** Urinary angiotensin-converting enzyme
 770 activity in type 2 diabetes mellitus: its relationship to diabetic nephropathy. *Acta*
 771 *diabetologica* 32: 193-197, 1995.
- 772 73. **Nerlich AG, Schleicher ED, Wiest I, Specks U, and Timpl R.** Immunohistochemical
 773 localization of collagen VI in diabetic glomeruli. *Kidney International* 45: 1648-1656, 1994.
- 774 74. **Noh H, and King GL.** The role of protein kinase C activation in diabetic
 775 nephropathy. *Kidney international Supplement* S49-53, 2007.
- 776 75. **Pantsulaia T.** Role of TGF-beta in pathogenesis of diabetic nephropathy. *Georgian*
 777 *medical news* 13-18, 2006.
- 778 76. **Paterson AD, Waggott D, Boright AP, Hosseini SM, Shen E, Sylvestre MP, Wong**
 779 **I, Bharaj B, Cleary PA, Lachin JM, Below JE, Nicolae D, Cox NJ, Canty AJ, Sun L, and Bull**
 780 **SB.** A genome-wide association study identifies a novel major locus for glycemic control in
 781 type 1 diabetes, as measured by both A1C and glucose. *Diabetes* 59: 539-549, 2010.
- 782 77. **Pesavento TE.** Kidney transplantation in the context of renal replacement therapy.
 783 *Clinical journal of the American Society of Nephrology : CJASN* 4: 2035-2039, 2009.
- 784 78. **Peti-Peterdi J.** High glucose and renin release: the role of succinate and GPR91.
 785 *Kidney Int* 78: 1214-1217, 2010.
- 786 79. **Pettersson US, Walden TB, Carlsson PO, Jansson L, and Phillipson M.** Female
 787 mice are protected against high-fat diet induced metabolic syndrome and increase the
 788 regulatory T cell population in adipose tissue. *PLOS ONE* 7: e46057, 2012.
- 789 80. **Ramos-Lopez O, Arpon A, Riezu-Boj JI, Milagro FI, Mansego ML, and Martinez**
 790 **JA.** DNA methylation patterns at sweet taste transducing genes are associated with BMI and
 791 carbohydrate intake in an adult population. *Appetite* 120: 230-239, 2017.
- 792 81. **Riazi S, Madala-Halagappa VK, Hu X, and Ecelbarger CA.** Sex and body-type
 793 interactions in the regulation of renal sodium transporter levels, urinary excretion, and
 794 activity in lean and obese Zucker rats. *Gender medicine* 3: 309-327, 2006.
- 795 82. **Rubin A, Salzberg AC, Imamura Y, Grivitishvili A, and Tombran-Tink J.**
 796 Identification of novel targets of diabetic nephropathy and PEDF peptide treatment using
 797 RNA-seq. *BMC genomics* 17: 936, 2016.
- 798 83. **Sakuma T, Honma R, Maguchi S, Tamaki H, and Nemoto N.** Different expression
 799 of hepatic and renal cytochrome P450s between the streptozotocin-induced diabetic
 800 mouse and rat. *Xenobiotica; the fate of foreign compounds in biological systems* 31: 223-237,
 801 2001.
- 802 84. **Schock-Kusch D, Geraci S, Ermeling E, Shulhevich Y, Sticht C, Hesser J,**
 803 **Stsepankou D, Neudecker S, Pill J, Schmitt R, and Melk A.** Reliability of Transcutaneous
 804 Measurement of Renal Function in Various Strains of Conscious Mice. *PLOS ONE* 8: e71519,
 805 2013.
- 806 85. **Schreiber A, Shulhevich Y, Geraci S, Hesser J, Stsepankou D, Neudecker S,**
 807 **Koenig S, Heinrich R, Hoecklin F, Pill J, Friedemann J, Schweda F, Gretz N, and Schock-**
 808 **Kusch D.** Transcutaneous measurement of renal function in conscious mice. *American*
 809 *Journal of Physiology - Renal Physiology* 303: F783, 2012.

- 810 86. **Shepard BD, Cheval L, Peterlin Z, Firestein S, Koepsell H, Doucet A, and**
811 **Pluznick JL.** A Renal Olfactory Receptor Aids in Kidney Glucose Handling. *Scientific Reports*
812 6: 35215, 2016.
- 813 87. **Shi X, Zhan L, Xiao C, Lei Z, Yang H, Wang L, Zhao J, and Zhang HT.** miR-1238
814 inhibits cell proliferation by targeting LHX2 in non-small cell lung cancer. *Oncotarget* 6:
815 19043-19054, 2015.
- 816 88. **Singec I, Knoth R, Ditter M, Hagemeier CE, Rosenbrock H, Frotscher M, and**
817 **Volk B.** Synaptic vesicle protein synaptoporin is differently expressed by subpopulations of
818 mouse hippocampal neurons. *The Journal of comparative neurology* 452: 139-153, 2002.
- 819 89. **Snel B, Lehmann G, Bork P, and Huynen MA.** STRING: a web-server to retrieve
820 and display the repeatedly occurring neighbourhood of a gene. *Nucleic acids research* 28:
821 3442-3444, 2000.
- 822 90. **Snyder EM, Nong Y, Almeida CG, Paul S, Moran T, Choi EY, Nairn AC, Salter MW,**
823 **Lombroso PJ, Gouras GK, and Greengard P.** Regulation of NMDA receptor trafficking by
824 amyloid-beta. *Nature neuroscience* 8: 1051-1058, 2005.
- 825 91. **Subramanian B, Ko WC, Yadav V, DesRochers TM, Perrone RD, Zhou J, and**
826 **Kaplan DL.** The regulation of cystogenesis in a tissue engineered kidney disease system by
827 abnormal matrix interactions. *Biomaterials* 33: 8383-8394, 2012.
- 828 92. **Sullivan JC, Pardieck JL, Hyndman KA, and Pollock JS.** Renal NOS activity,
829 expression, and localization in male and female spontaneously hypertensive rats. *American*
830 *journal of physiology Regulatory, integrative and comparative physiology* 298: R61-69, 2010.
- 831 93. **Surwit RS, Kuhn CM, Cochrane C, McCubbin JA, and Feinglos MN.** Diet-Induced
832 Type II Diabetes in C57BL/6J Mice. *Diabetes* 37: 1163, 1988.
- 833 94. **Szewczyk JR, and Laudeman C.** CCK1R agonists: a promising target for the
834 pharmacological treatment of obesity. *Current topics in medicinal chemistry* 3: 837-854,
835 2003.
- 836 95. **Szklarczyk D, Franceschini A, Wyder S, Forsslund K, Heller D, Huerta-Cepas J,**
837 **Simonovic M, Roth A, Santos A, Tsafou KP, Kuhn M, Bork P, Jensen LJ, and von Mering**
838 **C.** STRING v10: protein-protein interaction networks, integrated over the tree of life.
839 *Nucleic acids research* 43: D447-452, 2015.
- 840 96. **Tain YL, Hsu CN, Chan JY, and Huang LT.** Renal Transcriptome Analysis of
841 Programmed Hypertension Induced by Maternal Nutritional Insults. *International journal*
842 *of molecular sciences* 16: 17826-17837, 2015.
- 843 97. **Takahashi T, Abe H, Arai H, Matsubara T, Nagai K, Matsuura M, Iehara N,**
844 **Yokode M, Nishikawa S, Kita T, and Doi T.** Activation of STAT3/Smad1 is a key signaling
845 pathway for progression to glomerulosclerosis in experimental glomerulonephritis. *The*
846 *Journal of biological chemistry* 280: 7100-7106, 2005.
- 847 98. **Takahashi T, Tabuchi T, Tamaki Y, Kosaka K, Takikawa Y, and Satoh T.**
848 Carnosic acid and carnosol inhibit adipocyte differentiation in mouse 3T3-L1 cells through
849 induction of phase2 enzymes and activation of glutathione metabolism. *Biochemical and*
850 *biophysical research communications* 382: 549-554, 2009.
- 851 99. **Taylor LE, and Sullivan JC.** Sex Differences in Obesity-Induced Hypertension and
852 Vascular Dysfunction: A Protective Role for Estrogen in Adipose Tissue Inflammation?
853 *American journal of physiology Regulatory, integrative and comparative physiology ajpregu*
854 00202 02016, 2016.

- 855 100. **Tetlow N, and Board PG.** Functional polymorphism of human glutathione
856 transferase A2. *Pharmacogenetics* 14: 111-116, 2004.
- 857 101. **Toma I, xF, Kang JJ, Sipos A, Vargas S, Bansal E, Hanner F, Meer E, Peti-Peterdi J, xE, and nos.** Succinate receptor GPR91 provides a direct link between high glucose levels
858 and renin release in murine and rabbit kidney. *The Journal of clinical investigation* 118:
859 2526-2534, 2008.
- 860 102. **Tsukaguchi H, Shayakul C, Berger UV, and Hediger MA.** Urea transporters in
861 kidney: molecular analysis and contribution to the urinary concentrating process1. *The*
862 *American journal of physiology* 275: F319-324, 1998.
- 863 103. **Ustundag B, Canatan H, Cinkilinc N, Halifeoglu I, and Bahcecioglu IH.**
864 Angiotensin converting enzyme (ACE) activity levels in insulin-independent diabetes
865 mellitus and effect of ACE levels on diabetic patients with nephropathy. *Cell biochemistry*
866 *and function* 18: 23-28, 2000.
- 867 104. **Vaidya VS, Ferguson MA, and Bonventre JV.** Biomarkers of Acute Kidney Injury.
868 *Annual review of pharmacology and toxicology* 48: 463-493, 2008.
- 869 105. **Wang C-Y, and Liao JK.** A Mouse Model of Diet-Induced Obesity and Insulin
870 Resistance. *Methods in molecular biology (Clifton, NJ)* 821: 421-433, 2012.
- 871 106. **Wang J, Hu W, Li L, Huang X, Liu Y, Wang D, and Teng L.** Antidiabetic activities of
872 polysaccharides separated from Inonotus obliquus via the modulation of oxidative stress in
873 mice with streptozotocin-induced diabetes. *PLOS ONE* 12: e0180476, 2017.
- 874 107. **Wei P, Grimm PR, Settles DC, Balwanz CR, Padanilam BJ, and Sansom SC.**
875 Simvastatin reverses podocyte injury but not mesangial expansion in early stage type 2
876 diabetes mellitus. *Renal failure* 31: 503-513, 2009.
- 877 108. **Wei P, Lane PH, Lane JT, Padanilam BJ, and Sansom SC.** Glomerular structural
878 and functional changes in a high-fat diet mouse model of early-stage Type 2 diabetes.
879 *Diabetologia* 47: 1541-1549, 2004.
- 880 109. **Whaley-Connell A, and Sowers JR.** Obesity and kidney disease: from population to
881 basic science and the search for new therapeutic targets. *Kidney Int* 92: 313-323, 2017.
- 882 110. **Wickman C, and Kramer H.** Obesity and Kidney Disease: Potential Mechanisms.
883 *Seminars in nephrology* 33: 14-22, 2013.
- 884 111. **Wong N, Dontireddy L, Babu S, Adhikary D, Chakraborty S, and Chakraborty
885 T.** Differential effect of high fat diet on tissue morphology and hormonal levels in male and
886 female mice (765.1). *The FASEB Journal* 28: 2014.
- 887 112. **Wu B, Lu P, Cloer C, Shaban M, Grewal S, Milazi S, Shah SN, Moulton HM, and Lu
888 QL.** Long-term rescue of dystrophin expression and improvement in muscle pathology and
889 function in dystrophic mdx mice by peptide-conjugated morpholino. *Am J Pathol* 181: 392-
890 400, 2012.
- 891 113. **Wu HK, Heng HH, Siderovski DP, Dong WF, Okuno Y, Shi XM, Tsui LC, and
892 Minden MD.** Identification of a human LIM-Hox gene, hLH-2, aberrantly expressed in
893 chronic myelogenous leukaemia and located on 9q33-34.1. *Oncogene* 12: 1205-1212, 1996.
- 894 114. **Wu P, Ren Y, Ma Y, Wang Y, Jiang H, Chaudhari S, Davis ME, Zuckerman JE, and
895 Ma R.** Negative regulation of Smad1 pathway and collagen IV expression by store-operated
896 Ca²⁺ entry in glomerular mesangial cells. *American journal of physiology Renal physiology*
897 312: F1090-F1100, 2017.
- 898 115. **Wysocki J, Ye M, Soler MJ, Gurley SB, Xiao HD, Bernstein KE, Coffman TM, Chen
899 S, and Batlle D.** ACE and ACE2 activity in diabetic mice. *Diabetes* 55: 2132-2139, 2006.
- 900

- 901 116. **Yokoyama H, and Deckert T.** Central role of TGF-beta in the pathogenesis of
902 diabetic nephropathy and macrovascular complications: a hypothesis. *Diabetic medicine : a*
903 *journal of the British Diabetic Association* 13: 313-320, 1996.
- 904 117. **Yoshinari K, Takagi S, Sugatani J, and Miwa M.** Changes in the expression of
905 cytochromes P450 and nuclear receptors in the liver of genetically diabetic db/db mice.
906 *Biological & pharmaceutical bulletin* 29: 1634-1638, 2006.
- 907 118. **Yosten GL, Kolar GR, Redlinger LJ, and Samson WK.** Evidence for an interaction
908 between proinsulin C-peptide and GPR146. *The Journal of endocrinology* 218: B1-8, 2013.
- 909 119. **Zhu C, Hansen AR, Bateman T, Chen Z, Holt TG, Hubert JA, Karanam BV, Lee SJ,**
910 **Pan J, Qian S, Reddy VB, Reitman ML, Strack AM, Tong V, Weingarth DT, Wolff MS,**
911 **MacNeil DJ, Weber AE, Duffy JL, and Edmondson SD.** Discovery of imidazole
912 carboxamides as potent and selective CCK1R agonists. *Bioorganic & medicinal chemistry*
913 *letters* 18: 4393-4396, 2008.
- 914
- 915
- 916

917
918 **Figure 1. HF diet increases weight, glucose handling, and GFR in male mice.**
919 Significant increases were seen in weight at time of sacrifice in males and in weight-
920 matched females (A). Non-fasting blood glucose was significantly increased at sacrifice
921 only in the males (B). Male HF mice exhibited a significant decrease in glucose
922 tolerance (C, D; n=5 HF, n =4 Ctrl). GFR was significantly elevated in HF male mice (E;
923 n=4 HF, n=4 Ctrl). Open symbols represent control fed animals while filled symbols
924 represent high fat fed animals. * p < 0.05 high fat vs control by t-test. For A, B, and E
925 the n of each group is indicated by the number of points plotted. The prime symbol (')
926 denotes the weight-matched female group.

927

928

929

930
931 **Figure 2. Renal Histology of HF mice.** Representative H&E images are shown from
932 male Ctrl (A) and HF (B) renal cortex sections, demonstrating glomerular size trending
933 toward an increase in HF animals, as shown in C (n=4-5 mice per group, with >60
934 glomeruli per group in total). Picosirius red images from both Ctrl (D) and HF (E)
935 sections are shown, with glomerular collagen fraction was quantified in panel F (n=4
936 mice per group, with >120 glomeruli per group in total). Additionally, Collagen IV
937 immunohistochemical stains are shown from both Ctrl (G) and HF (H) sections, with
938 total Collagen IV signal was quantified in panel I (n=4 mice per group with >50 fields of
939 view per group). KIM-1 immunohistochemical stains are shown for both Ctrl (J) and HF
940 (K) sections. Finally, Western blots (L) are shown for KIM-1 and GAPDH, for both Ctrl
941 and HF kidneys as well as (+) control kidneys subjected to ischemia-reperfusion injury.
942 Scale bars represent 50 μ m.

943

944

945

946

947
948 **Figure 3. Comparison of Fold Change by RNASeq versus qRT-PCR.** A comparison
949 of fold change values in the renal cortex (Cx) between RNA Seq data (light gray) and
950 qRT-PCR data (dark gray) for genes with (A) greatest fold increase, (B) greatest fold
951 decrease, and (C) other genes of interest. n=5 for qRT-PCR, except where indicated by
952 # (n=4). # indicates significance by both RNASeq (rsem-run-ebseq, rsem-control-FDR
953 < 0.05) and qRT-PCR (ANOVA); the lack of symbol indicates data are significant by
954 RNASeq only.
955

956
957 **Table 1. KEGG Pathways.** 353 genes clustered into various KEGG pathways.
958 Pathways that included more than one gene are listed for 17 pathways total. KEGG
959 pathways are listed with the total number of genes clustered into that pathway, as well
960 as the number of genes up-regulated, or down-regulated. Bold indicates genes with
961 most extreme fold changes.
962

963
964 **Table 2. Differentially Expressed Genes via RNA Seq.** The top 11 genes differentially
965 expressed in male renal cortex in each category are listed by fold change (HF/Ctrl; false
966 discovery rate < 0.05, p<0.05, n=4 mice per group).

967

968

969 **Table 3. Confirmation of Differentially Expressed Genes via qRT-PCR.** Fold change970 was calculated as $2^{(-\Delta\Delta Ct)}$. *Equal variance test failed, significant by T-Test. N.S.,

971 non-significant. n=5 per group (genes marked with an # n=4 in cortex). + the probe for

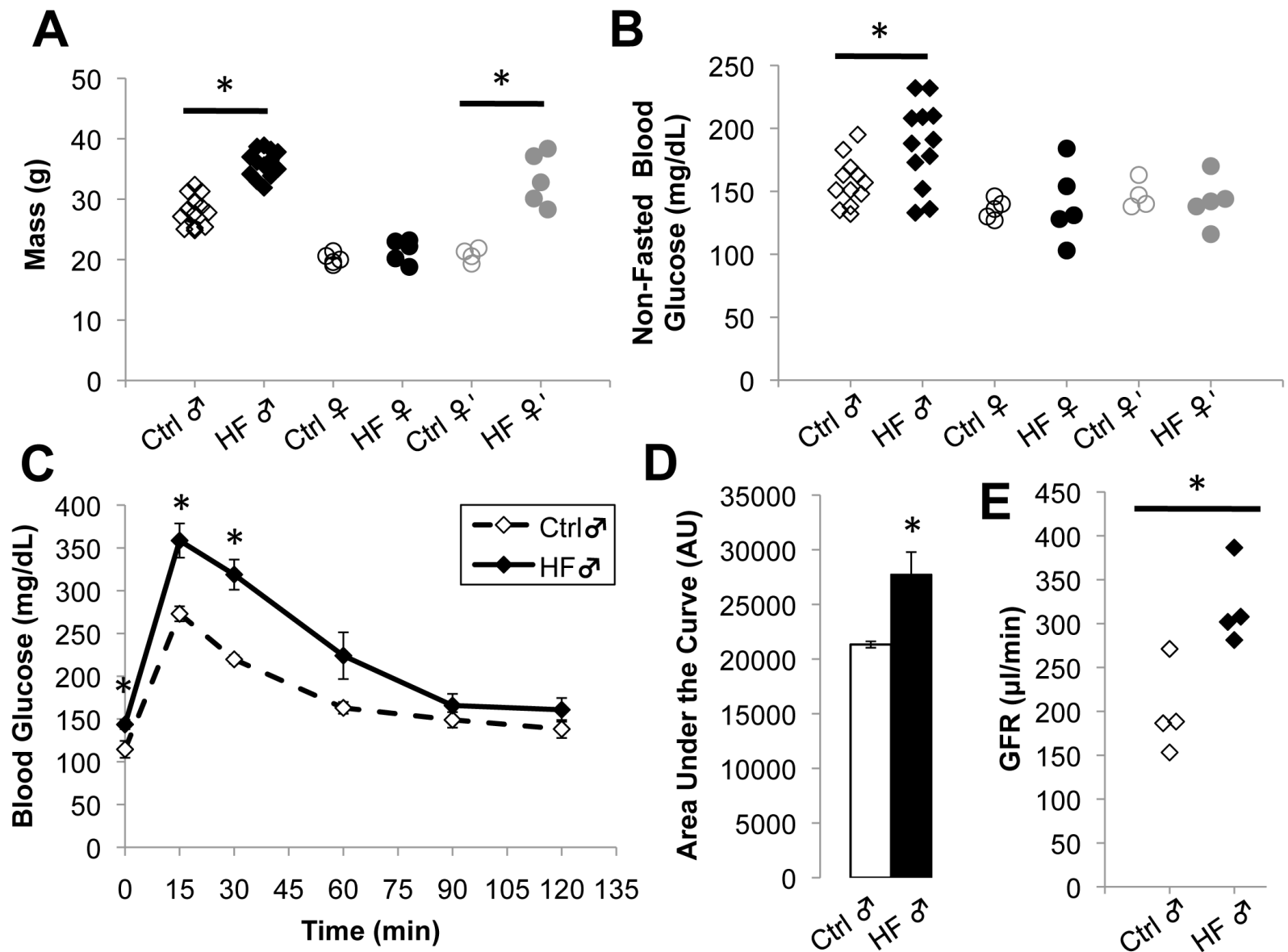
972 Cyp2a5 also recognizes Cyp2a4.

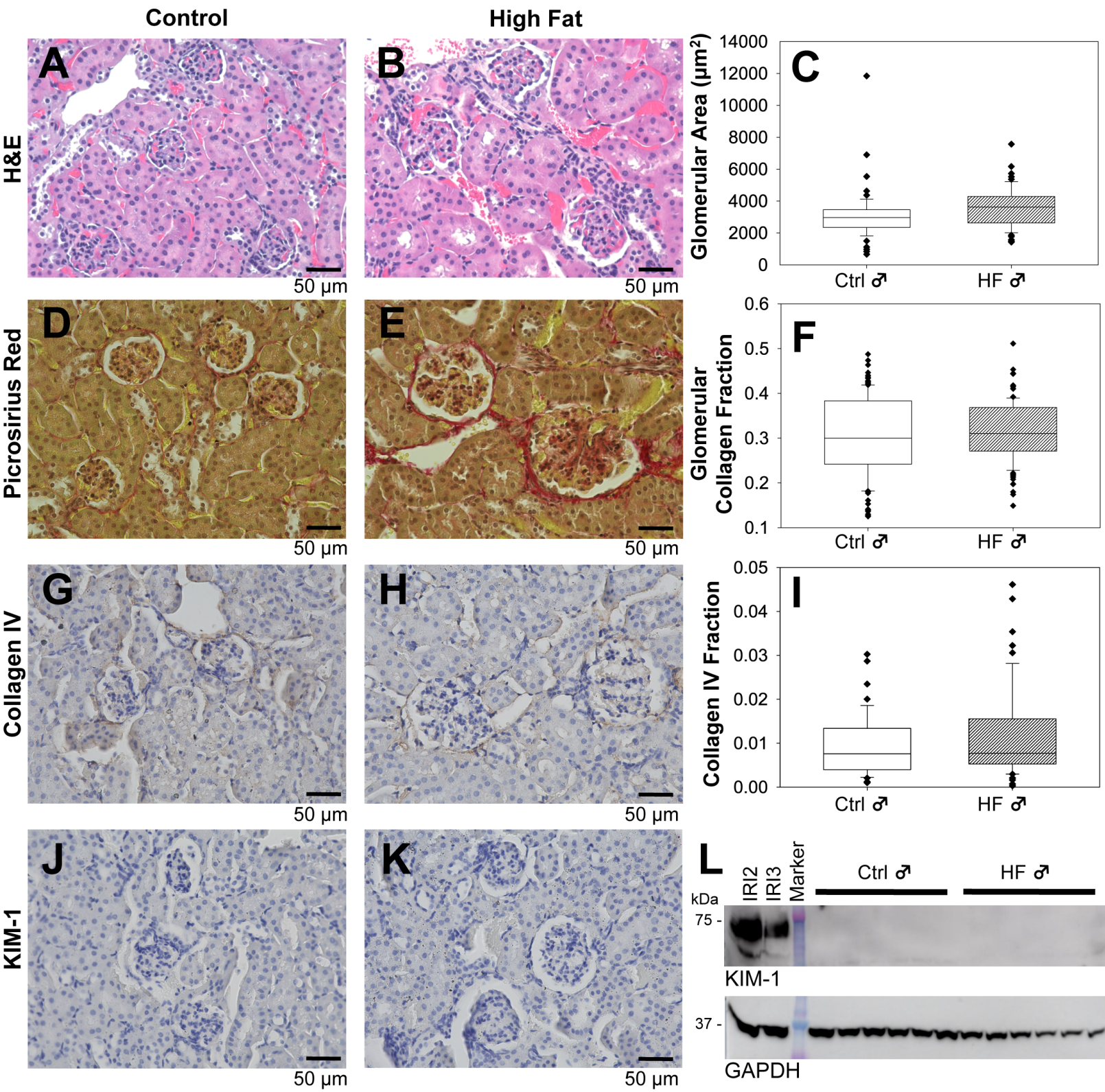
973

974
975 **Table 4. Expanded Tissue qRT-PCR Screen.** Tissue specific expression of the 11
976 genes that were confirmed by qRT-PCR. Solid arrows represent $p < 0.05$ by one way
977 ANOVA for male cortex and medulla samples, or by Student's T Test (Ctrl vs HF) for all
978 other tissues. Open arrows demonstrate trends that fail to reach significance. The size
979 of the arrow indicates the magnitude of the change, shown in the lower right-hand
980 corner. \wedge , expressed in high fat samples only; \vee , expressed in control samples only;
981 N.D., not detected in any sample. Data unreliable indicates inconsistent technical
982 replicates. Females: DM, diet matched, WM', weight matched.

983

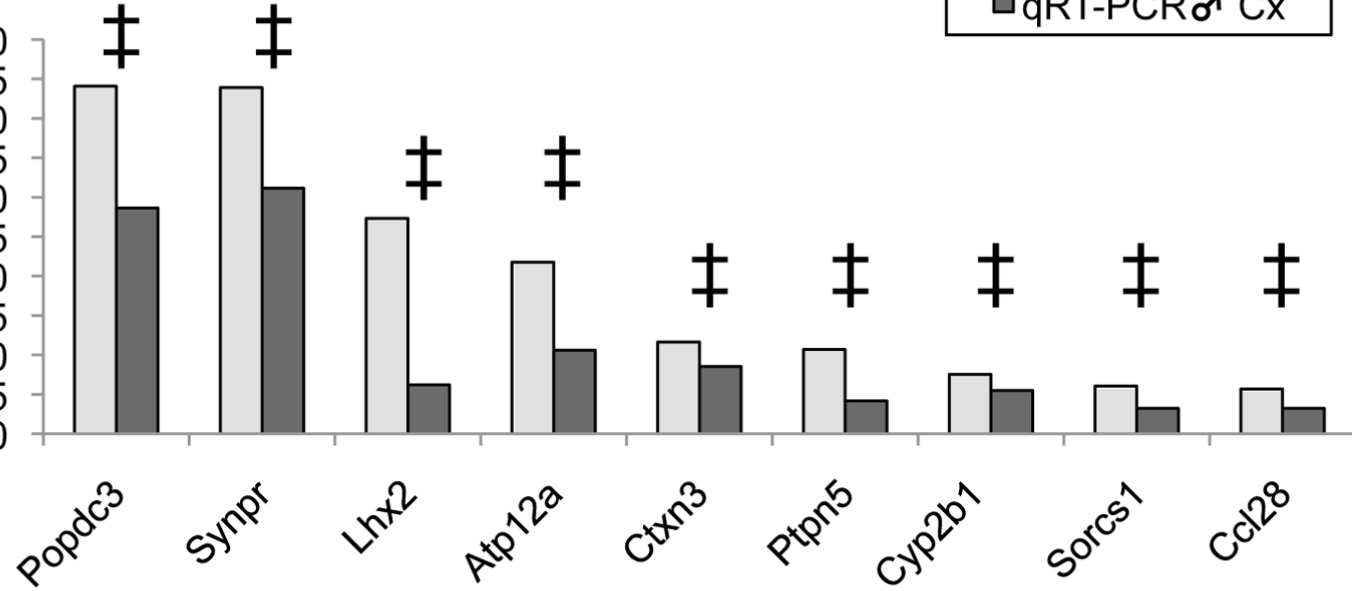
984
985



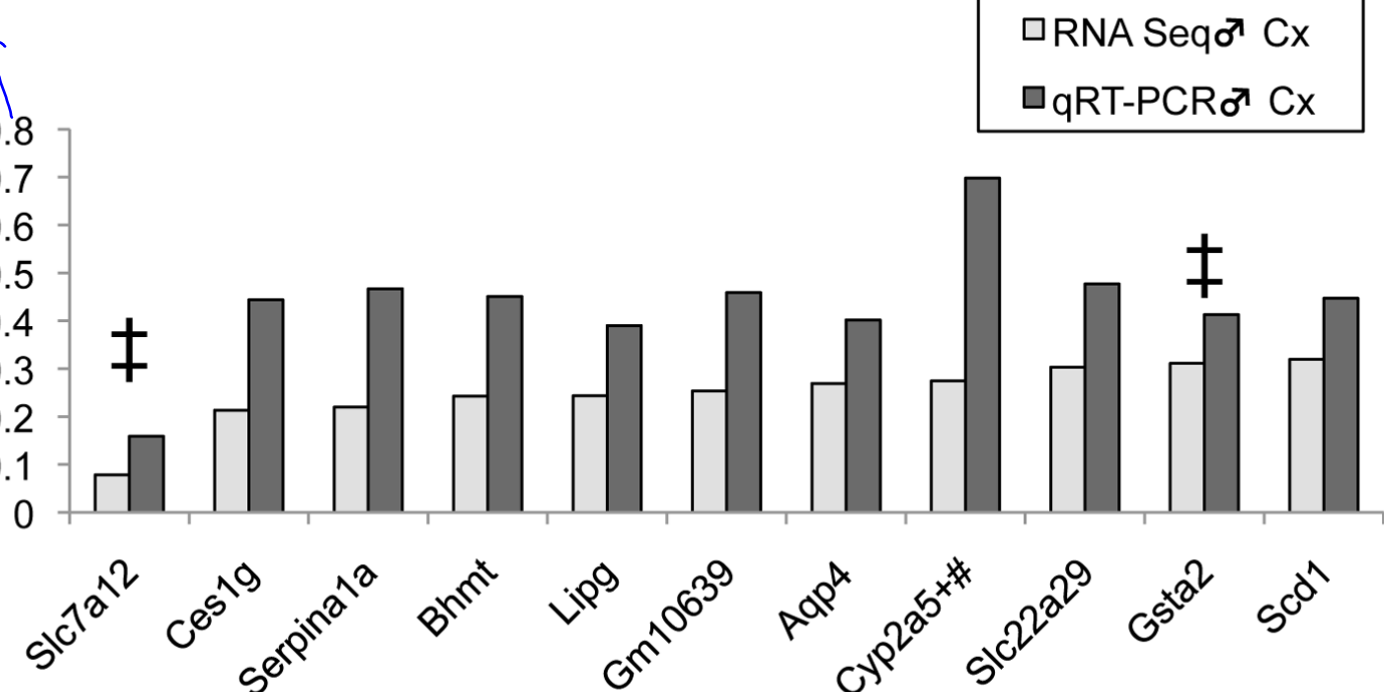


A

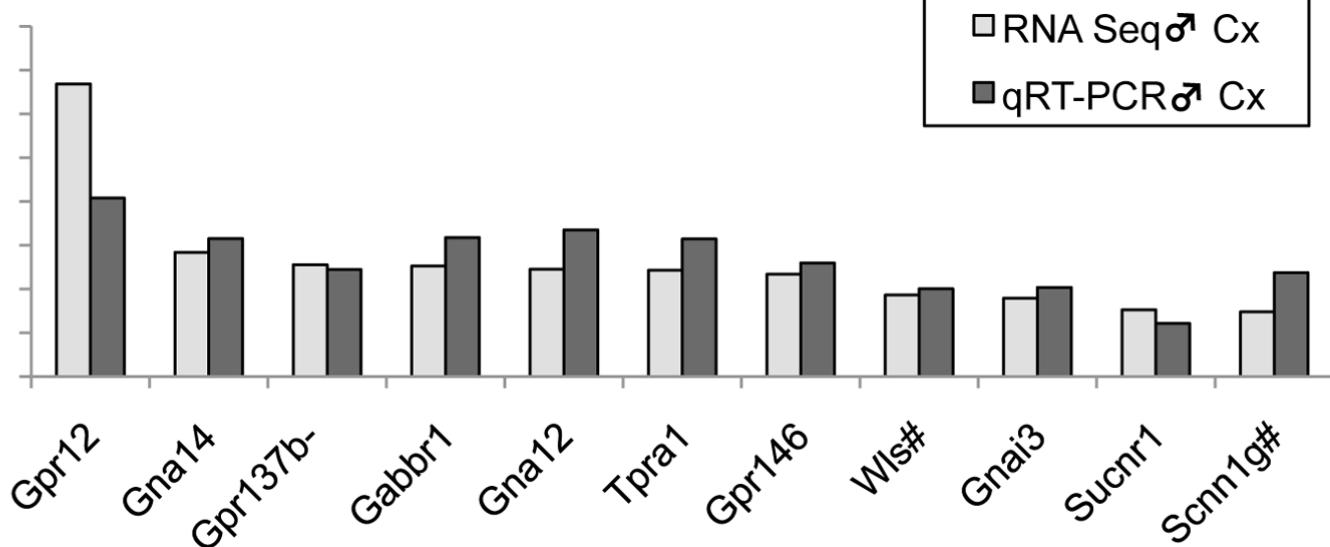
Fold Change (HF/Ctrl)

**B**

Fold Change (HF/Ctrl)

**C**

Fold Change (HF/Ctrl)



KEGG Pathway	DEGs Total	DEGs ↑	DEGs ↓	↑ Genes	↓ Genes
Spliceosome	19	0	19	(N/A)	MAGOH, HSPA1A, SNW1, SF3B3, SF3A3, PRPF19, SF3B1, HNRNPM, HNRNPK, SNRNPB, DHX15, LSM3, SNRNP70, HNRNPC, PHF5A, SNRNP27, HSPA8, PUF60, SNRPG
Glutathione metabolism	15	3	12	GGT1, GPX1, OPLAH	GSTA2 , GSTA3, GSTA4, G6PDX, GCLM, GSTM7, GSTM1, GSR, GSTM4, GPX6, GSTK1, GSTP1
Drug metabolism	15	3	12	CYP2E1, CYP2B10 , FMO5	GSTA2 , GSTA3, GSTA4, CYP2C44, UGT1A1, GSTM7, GSTM1, GSTM4, UGT1A2, UGT1A6B, GSTK1, CYP2A5 , GSTP1, CYP2A4
PPAR signaling pathway	14	8	6	ACOX1, PPARA, CPT2, CPT1A, ACOX3, PCK1, CYP4A12A, CYP4A32,	ACOX2, SCD1 , SCD2, FADS2, ILK, FABP7
Metabolism of xenobiotics by cytochrome P450	12	2	10	CYP2E1, CYP2B10	GSTM1, GSTA2 , GSTA3, GSTM4, GSTA4, CYP2C44, UGT1A6B, UGT1A2, GSTK1, UGT1A1, GSTP1, GSTM7
Arachidonic acid metabolism	11	8	3	GPX1, CYP4A12A, TBXAS1, CYP4A32, CYP2J9, GGT1, CYP2E1, CYP2B10	CYP2C44, GPX6, LTA4H
ErbB signaling pathway	11	7	4	PRKCA, ERBB3, STAT5A, STAT5B, HBEGF, MTOR, SRC	PAK6, PTK2, ERBB4, PLCG2
Fatty acid metabolism	9	8	1	ACOX1, CYP4A12A, CPT2, CYP4A32, ACADS, ALDH3A2, CPT1A, ACOX3	ACADSB
Biosynthesis of unsaturated fatty acids	8	3	5	ACOX1, PTPLB, ACOX3	SCD1 , SCD2, FADS1, FADS2, ELOVL6
ABC transporters	8	1	7	ABCA1	ABCC9, ABCB1A, ABCB1B, ABCC4, CFTR, ABCC1, ABCA13
Glycine, serine and threonine metabolism	7	1	6	CHDH	CTH, AMT, BHMT, GCAT, DMGDH, GNMT
Valine, leucine and isoleucine degradation	7	4	3	BCKDHA, ALDH6A1, ACADS, ALDH3A2	DBT, ACADSB, ABAT
Butanoate metabolism	6	4	2	ACSM3, ACSM2, ACADS, ALDH3A2	ABAT, AKR1C13
Pentose phosphate pathway	5	0	5	(N/A)	RPE, G6PDX, PFKP, TKT, FBP2
Renin-angiotensin system	5	3	2	ACE, MAS1, CTSA	MME, ENPEP
Terpenoid backbone biosynthesis	4	0	4	(N/A)	HMGCR, FDPS, MVK, IDI1
Other glycan degradation	4	4	0	NEU1, FUCA2, FUCA1, GLB1	(N/A)

353 genes clustered into various KEGG pathways. Pathways that included more than one gene are listed for 17 pathways total. KEGG pathways are listed with the total number of genes clustered into that pathway, as well as the number of genes up-regulated, or down-regulated. Bold indicates genes with most extreme fold changes.

Gene	Fold Δ	PPEE	PPDE	Ctrl FPKM (Mean ± SEM)	HF FPKM (Mean ± SEM)
A. Genes with Greatest Fold Increase					
Popdc3	44.1	6.94E-08	1.00	0.025 ± 0.010	0.988 ± 0.268
Synpr	43.9	2.10E-06	1.00	0.195 ± 0.098	7.955 ± 3.780
Lhx2	27.3	4.08E-02	0.96	0.003 ± 0.003	0.093 ± 0.035
Atp12a	21.8	9.51E-05	1.00	0.025 ± 0.018	0.535 ± 0.160
Gm14435	13.8	1.80E-03	1.00	0.095 ± 0.033	1.755 ± 1.057
Ctxn3	11.7	0.00	1.00	1.373 ± 0.619	15.300 ± 2.207
Ptpn5	10.7	4.59E-03	1.00	0.005 ± 0.003	0.090 ± 0.030
Cyp2b10	7.5	1.17E-05	1.00	0.285 ± 0.144	2.143 ± 0.471
Sorcs1	6.1	1.81E-05	1.00	0.065 ± 0.027	0.373 ± 0.073
Gm15441	5.9	1.95E-02	0.98	0.693 ± 0.230	4.073 ± 1.114
Ccl28	5.7	2.12E-03	1.00	2.405 ± 1.059	13.115 ± 2.846
B. Genes with Greatest Fold Decrease					
Slc7a12	0.08	3.68E-04	1.00	3.595 ± 0.498	0.343 ± 0.061
Ces1g	0.2	4.28E-05	1.00	6.403 ± 1.270	1.513 ± 0.169
Serpina1a	0.2	0.00	1.00	6.343 ± 0.886	1.515 ± 0.360
Bhmt	0.2	8.33E-15	1.00	3.258 ± 0.432	0.860 ± 0.081
Lipg	0.2	4.33E-09	1.00	0.620 ± 0.084	0.170 ± 0.025
Gm10639	0.3	1.47E-06	1.00	4.868 ± 0.658	1.383 ± 0.154
Aqp4	0.3	4.72E-10	1.00	2.825 ± 0.460	0.833 ± 0.192
Cyp2a5	0.3	1.61E-05	1.00	175.723 ± 26.088	53.325 ± 6.185
Slc22a29	0.3	9.67E-05	1.00	2.155 ± 0.485	0.688 ± 0.077
Gsta2	0.3	1.04E-05	1.00	242.055 ± 36.731	82.810 ± 6.919
Scd1	0.3	0.00	1.00	15.340 ± 2.399	5.178 ± 0.675
C. Other Genes of Interest					
Gpr12	3.3	6.77E-03	0.99	0.078 ± 0.018	0.268 ± 0.048
Gna14 (Gα14)	1.4	5.38E-06	1.00	6.515 ± 1.113	9.655 ± 0.422
Gpr137b-ps	1.3	1.32E-02	0.99	24.358 ± 4.299	32.628 ± 1.955
Gabbr1	1.3	4.58E-03	1.00	1.925 ± 0.314	2.568 ± 0.160
Gna12 (Gα12)	1.2	4.12E-07	1.00	37.708 ± 5.836	49.080 ± 1.521
Tpra1(Gpr175)	1.2	2.77E-05	1.00	11.488 ± 1.957	14.625 ± 0.441
Gpr146	1.2	2.31E-05	1.00	12.590 ± 2.024	15.528 ± 0.749
Wls (Gpr177)	0.9	2.90E-06	1.00	73.365 ± 12.181	71.680 ± 1.474
Gnai3 (Gi3)	0.9	1.54E-03	1.00	36.440 ± 6.341	34.038 ± 1.155
Sucnr1 (Gpr91)	0.8	8.11E-06	1.00	34.500 ± 6.511	27.053 ± 0.684
Scnn1g (ENaC γ)	0.7	4.57E-12	1.00	17.928 ± 2.673	14.098 ± 0.526

The top 11 genes differentially expressed in male renal cortex in each category are listed by fold change (HF/Ctrl; false discovery rate < 0.05, p<0.05, n=4 mice per group).

Gene	Fold Δ	Ctrl ΔCT (Mean ± SEM)	HF ΔCT (Mean ± SEM)	Significance	Assay #
<u>A. Genes with Greatest Fold Increase</u>					
Popdc3	28.6	23.0 ± 0.8	18.2 ± 0.7	p = 0.002	Mm00712331_m1
Synpr	31.2	20.5 ± 0.9	15.6 ± 0.7	p < 0.001	Mm00511114_m1
Lhx2	6.2	23.1 ± 0.5	20.5 ± 0.6	p = 0.013*	Mm00839783_m1
Atp12a	10.6	23.0 ± 0.5	19.6 ± 0.8	p = 0.005	Mm01318023_m1
Ctxn3	8.5	18.7 ± 0.5	15.5 ± 0.4	p < 0.001	Mm01718023_m1
Ptpn5	4.2	24.6 ± 0.4	22.5 ± 0.6	p = 0.007	Mm00479063_m1
Cyp2b10	5.5	19.2 ± 0.4	16.8 ± 0.6	p = 0.005	Mm01972453_s1
Sorcs1	3.2	21.4 ± 0.4	19.7 ± 0.6	p = 0.003	Mm00491259_m1
Ccl28	3.2	17.5 ± 0.6	15.8 ± 0.2	p = 0.028	Mm00445039_m1
<u>B. Genes with Greatest Fold Decrease</u>					
Slc7a12	0.2	16.8 ± 0.3	19.5 ± 0.4	p < 0.001	Mm00499866_m1
Cesg1	0.4	16.4 ± 0.5	17.6 ± 0.6	N.S.	Mm00491334_m1
Serpina1a	0.5	22.5 ± 1.0	23.7 ± 0.5	N.S.	Mm02748447_g1
Bhmt	0.5	17.6 ± 0.3	18.7 ± 0.6	N.S.	Mm04210521_g1
Lipg	0.4	20.8 ± 0.4	22.1 ± 0.6	N.S.	Mm00495368_m1
Gm10639	0.5	12.3 ± 0.3	13.5 ± 0.6	N.S.	Mm03647534_u1
Aqp4	0.4	17.2 ± 0.5	18.5 ± 0.9	N.S.	Mm00802131_m1
Cyp2a5+#+	0.7	10.9 ± 0.5	11.4 ± 0.6	N.S.	Mm00487248_g1
Slc22a29	0.5	20.7 ± 0.3	21.8 ± 0.6	N.S.	Mm00655572_mH
Gsta2	0.4	11.2 ± 0.3	12.5 ± 0.6	p = 0.027	Mm03019257_g1
Scd1	0.4	14.9 ± 0.5	16.1 ± 0.6	N.S.	Mm00772290_m1
<u>C. Other Genes of Interest</u>					
Gpr12	2.0	22.8 ± 0.5	21.7 ± 0.5	N.S.	Mm02343663_s1
Gna14 (Gα14)	1.6	17.3 ± 0.6	17.1 ± 0.4	N.S.	Mm00492374_m1
Gpr137b-ps#	1.2	15.7 ± 0.3	15.4 ± 0.6	N.S.	Mm01620949_s1
Gabbr1	1.6	16.9 ± 0.4	16.3 ± 0.7	N.S.	Mm00444578_m1
Gna12 (Gα12)	1.7	13.5 ± 0.5	13.4 ± 0.5	N.S.	Mm00494665_m1
Tpra1(Gpr175)	1.6	18.5 ± 0.4	17.8 ± 0.5	N.S.	Mm01183739_m1
Gpr146	1.3	15.0 ± 0.3	14.6 ± 0.5	N.S.	Mm01951835_s1
Wls (Gpr177)#+	1.0	13.0 ± 0.3	13.0 ± 0.5	N.S.	Mm00509695_m1
Gnai3 (Gi3)	1.0	13.9 ± 0.5	14.1 ± 0.4	N.S.	Mm00802670_m1
Sucnr1 (Gpr91)	0.6	13.3 ± 0.2	14.0 ± 0.4	N.S.	Mm02620543_s1
Scnn1g (ENaC γ)#+	1.2	15.1 ± 0.4	14.9 ± 0.8	N.S.	Mm00441228_m1

Fold change was calculated as $2^{(-\Delta\Delta Ct)}$. *Equal variance test failed, significant by T-Test. N.S., non-significant. n=5 per group (genes marked with an # n=4 in cortex). + the probe for Cyp2a5 also recognizes Cyp2a4.

Fold Δs:	RNA Seq	quantitative RT-PCR					
Gene	♂ Cortex (n=4)	♂ Cortex (n=5)	♂ Medulla (n=3)	♂ Heart (n=3)	♂ Liver (n=3)	♀ Cortex DM	♀ Cortex WM'
Popdc3	↑ 44.1	↑ 28.6	↑ 11.8		↓ 1.6	↓ 0.1	0.8 0.5
Synpr	↑ 43.9	↑ 31.2	↑ 5.2	↓ 0.01	Λ N/A	1.4 N/A	4.1 N/A
Lhx2	↑ 27.3	↑ 6.2		↑ 1.1	↑ 2.3	0.7 N.D.	1.2 1.0
Atp12a	↑ 21.8	↑ 10.6	↑ 4.6	∨ N/A		1.3 N.D.	0.5 N.D.
Ctxn3	↑ 11.7	↑ 8.5	↑ 4.0	Λ N/A		1.9 N.D.	1.6 N.D.
Ptpn5	↑ 10.7	↑ 4.2	↑ 2.0	∨ N/A	↓ 3.5	↑ 2.1	0.7 N.D.
Cyp2b10	↑ 7.5	↑ 5.5	↑ 3.1	↑ 2.8	↑ 4.2	↑ 3.7	↓ 0.4
Sorcs1	↑ 6.1	↑ 3.2		1.0 1.8		N.D. 1.1	0.8 N.D.
Ccl28	↑ 5.7	↑ 3.2		1.5 0.9		1.0 2.5	0.6 N.D.
Slc7a12	↓ 0.08	↓ 0.2	↓ 0.1	∨ N/A	Data Unreliable	0.8 N.D.	1.0 N.D.
Gsta2	↓ 0.3	↓ 0.4	↓ 0.2	↑ 2.2	↓ 0.4	0.8 N.D.	0.8 N.D.

Tissue specific expression of the 11 genes that were confirmed by qRT-PCR. Solid arrows represent $p < 0.05$ by one way ANOVA for male cortex and medulla samples, or by Student's T Test (Ctrl vs HF) for all other tissues. Open arrows demonstrate trends that fail to reach significance. The size of the arrow indicates the magnitude of the change, shown in the lower right-hand corner. Λ, expressed in high fat samples only; ∨, expressed in control samples only; N.D., not detected in any sample. Data unreliable indicates inconsistent technical replicates. Females: DM, diet matched, WM', weight matched.